North Dakota Geological Survey

An Evaluation of the Resource Potential of the Tyler Formation (Pennsylvanian) using a Basin Centered Petroleum Accumulation Model

By

Stephan H. Nordeng and Timothy O. Nesheim

Figures

Tables

Executive Summary

The Tyler Formation (Lower Pennsylvanian) is a regionally extensive, organic rich unit that contains, over a significant part of its range, good to excellent quantities of kerogen. The richest kerogen is situated in the deepest portion of the Willston Basin (McKenzie County) and consists of marine derived organic matter that is prone to producing both oil and gas. Less rich kerogen is present along the flanks of the basin. This kerogen is dominated by terrestrial organic matter that is more likely to generate gas. A basin maturation model calibrated with experimentally derived kinetics and log based thermal stratigraphy indicate that there are two and possibly three portions of the Williston Basin in which the Tyler Formation is currently within the oil window. T_{max} values obtained from Rock Eval 6 analysis and the distribution of high resistivity shale are consistent with the maturation trends detailed by the basin analysis. Two of the areas that exhibit thermal maturity include known economic and sub-economic oil production, some of which is associated with over-pressurized formation fluids. The combination of organic rich source beds, thermal maturity and over-pressurized conditions is consistent with the basic requirements for a basin centered petroleum accumulation similar to the Bakken Formation. Unlike the Bakken, a sufficiently thick and laterally consistent reservoir has not been identified that would allow for the routine installation of horizontal well bores. However, additional work may find suitable targets in and adjacent to known sandstone reservoirs or in mechanically competent, units in the overlying upper Tyler Formation or underlying Otter Formation.

Introduction

The discovery and exploitation of the Bakken source system within the Williston Basin provides an excellent example of the parameters that may be used to explore for other similar resources (Nordeng et al., 2010). In particular, there are five factors of which four are principally geologic in nature that might prove useful in an exploration program. The first factor is provided by depositional settings conducive to the formation and preservation of a organic-rich source rock. The second element involves establishing the level of maturity that a given source rock has achieved. This involves reconstructing the thermal history of the source rock which together with the richness and type of kerogen involved can be used to evaluate whether or not the source rock has generated significant quantities of oil or gas or some combination of the two. The third element keys in on the expulsion of petroleum from the source beds into adjacent rocks. The fourth component is controlled by the permeability and porosity of the adjacent rocks. When permeabilities are very low, expulsion of oil from source beds will result in a petroleum accumulation that is unable to migrate away from the source beds. This process often produces abnormally high formation pressures (Schmoker, 2002). In addition to preventing migration, the reservoir units in this type of petroleum accumulation should also be sufficiently thick, laterally continuous and mechanically competent to accommodate the installation and stimulation of long horizontal well bores. This fifth element is primarily a function of the engineering requirements needed to successfully drill and complete productive wells.

The Tyler Formation is one of the youngest oil producing formations in the Williston Basin. A survey of the literature as well as conventional oil production from the interval suggests that the Tyler Formation may be capable of forming a basin centered oil accumulation similar in style to the Bakken Formation.

1) **Depositional setting**

The Tyler Formation in the Williston Basin of North Dakota was deposited during the Early Pennsylvanian Period (Ziebarth, 1962; Grenda, 1977) in a very shallow intracratonic basin that was connected to the Antler foredeep by the westward trending Big Snowy Trough (Peterson, 1981, Dorobek et al., 1991). Prior to Tyler deposition the entire basin was exposed resulting in an angular unconformity between the underlying Big Snowy Group and the overlying Tyler Formation (Fig. 1.1). Rocks contained in the Tyler Formation record a single, long-term retreat and advance in sea-level that culminates in the Permian with the deposition of the Amsden Formation (Gerhard and Anderson, 1988). There are at least ten transgressive events superimposed on this longer term sea level excursion with eight of these being present in the Medora Field (Barwis, 1990). These transgressive events are believed to be driven by high frequency oscillations in sea level that were superimposed upon the overall retreat of the Absoraka seas. However, throughout much of the Williston Basin only three of these cycles are documented (Foster, 1956; Willis, 1959; Maughan, 1984; Sturm, 1987).

During the early Pennsylvanian, the repeated growth and retreat of continental ice sheets spanning 10's to 100's of thousands of years caused sea level excursions on the order of 10s of meters (Heckel, 1994). These high frequency fluctuations in sea level produced complex and thinly bedded stratigraphic assemblages consisting of facies that range from off-shore marine through near-shore terrestrial deposits. Local variations in water depth induced by tectonic subsidence, uplift, sediment compaction and deposition further complicate the stratigraphic picture.

Lithologies commonly present in the terrestrial facies include sandstone, siltstone, shale, fresh water limestone, paleosols and coal. The marine environments include black, fissile shale, limestone, and gray shale that usually coarsens upsection. The exact vertical sequence and thicknesses of individual lithologies depends on the duration of the cycle, rates of sedimentation and the amount of accommodation space that is available during the cycle period. Obviously, longer period cycles are more likely to coincide with the formation of accommodation space through tectonic subsidence or sediment compaction than are shorter term cycles. The combination of gentle paleoslopes and comparatively large changes in sea-level generates a full, though highly variable, set of marine to continental lithofacies that are, at most, tens of feet thick.

 The organic-rich, radioactive shales situated within the deepest portion of the basin cover progressively smaller portions of the basin up section (Fig. 1.2). The interval containing these black shales is overlain by a regressive section dominated by oxidized red beds containing thin anhydrite beds. The sequence of lithologies suggests that during early Tyler time, accommodation space was provided by basin subsidence. During at least three major transgressive phases bottom waters near the center of the basin became sufficiently depleted in oxygen to allow significant amounts of organic carbon to be preserved. During the intervening regressive phases, sea level dropped enough to form paleosols, incised valleys later filled with sandstone and the occasional very thin coal. As the basin filled, subsidence in the central basin apparently failed to keep pace with the long-term fall in the Absaroka

sea level. In response to the diminished accommodation space, the central portion of the basin no longer was capable of forming organic-rich shale (See Fig. 1.3). However, organic-rich shale continued to be deposited along the southern flank of the basin. This change in the distribution of organic-rich shale could reflect a southward migration of the basins subsidence center. However, these organic-rich shales could be fresh or brackish water deposits that accumulated within a broad paleovalley that drained the delta/coastal plain facies tract directly into the Montana Trough (Sturm, 1987). Reduced accommodation space during the latter phase of Tyler deposition is suggested by the replacement of the organic-rich, transgressive shale facies by shallow water and anhydrite bearing terrestrial facies containing much less organic carbon. These overlying terrestrial sediments, in addition to recording a loss of accommodation space, may also coincide with a climate shift towards more arid conditions that resulted in extensive oxidation and the formation of the widespread anhydrite bearing red beds found in the upper portion of the Tyler throughout the central portion of the basin.

Within each cycle there are two or three lithofacies that may allow for the deposition and preservation of significant amounts of organic matter.   These lithofacies include an offshore marine facies formed during rising sea levels and two brackish to fresh water facies that represent progradational or retrogradation facies associated with falling sea levels.

In the case of the marine lithofacies, significant quantities of locally derived marine organic matter as well as terrestrial organic matter accumulates in offshore waters during the transgressive phase of each sea level cycle.   The preservation and accumulation of this material occurs when mixing within the water column is poor. Large amounts of organic detritus coupled with poor mixing may lead to anoxic or near anoxic conditions that results in the accumulation and possible burial of organic matter.   During trangressive phases, terrestrial sediment input is greatly diminished so that the accumulation of marine organic matter, undiluted by other sediment, results in abnormally rich total organic contents (TOC).   In addition, the absence or near absence of bottom water oxygen results in the precipitation and accumulation of relatively high concentrations of uranium compounds which produce intense responses on gamma ray logs. This association of organic and uranium rich sediments means that the gamma ray response may be helpful in identifying potential source rocks.

Marine organic matter is dominated by lipid compounds derived from planktonic organisms that lived in the well-oxygenated upper portion of the water column. The kerogen produced from this material (Type II) contains substantially more hydrogen bonded carbon than it does oxygen bonded carbon. Maturation of marine derived kerogen may produce oil, gas or some combination of the two.

Organic matter within the continental lithofacies accumulates primarily in anoxic fresh to brackish water marshes and lakes that develop on coastal and deltaic plains. Organic matter in these settings is often in the form of coal derived from terrestrial land plants. The kerogen (Type III) in coals usually contains relatively small amounts of hydrogen-bonded carbon and relatively high concentrations of hydrocarbon bonded oxygen. Generally, this kerogen generates gas and is not usually considered a source of liquid hydrocarbons. Less commonly, organic matter derived from lacustrine algae and cyanobacteria may also be important sources of organic carbon. The kerogen developed from these sources (Type I) contains substantially more hydrogen bonded carbon than is usually found in coal. This large hydrogen

component makes Type I kerogen far more likely to generate liquid petroleum (oil) than gas and in many cases the oil generated is rich in paraffin (Hedberg, H. D., 1968).

Coal and especially the associated paleosols mark the upper depositional limit of a single cycle.   During transgressive phases, marine sediments onlap these terrestrial environments and may result in the deposition of marine limestone, or deeper water, organic-rich shale directly on the upperrmost coal or paleosol of the previous cycle.   However, during the regressive phase or in response to deltaic progradation, marsh and delta plain lithofacies prograde seaward over deeper water lithofacies.

The significance of this depositional model with regard to the formation of petroleum source beds is that these "cycles" include continental and marine lithofacies that contain significant quantities of organic carbon. Even though individual source beds are thin, the accumulated thickness of these beds over several depositional cycles results in a significant source of organic carbon that makes the Tyler Formation an attractive candidate for a regional scale petroleum resource study.

Three regional scale facies tracts are evident within the Tyler Formation of North Dakota (Fig. 1.3). These include a central basin, transitional shoreline and deltaic or coastal plain facies.   Fossil assemblages in the central basin of McKenzie County include *Eolissochonetes* and *Aviculopecten eaglensis*. These assemblages are consistent with fluctuating open marine water depths (Grenda, 1977). Wireline logs of the central basin facies typically contain at least three persistent intervals containing thin (< 10 ft.), radioactive, organic-rich shale (see Fig. 1.1). Updip these radioactive shales grade into less radioactive shale that contain thin (<20 ft.) discontinuous, lenticular sand bodies that form the reservoir for most of the known Tyler production.   Fossils consistent with a transition from open marine to terrestrial conditions (Ziebarth ,1962; Grenda, 1977) include fresh water ostracods, *Lingula* (shoreline to deeper water, brackish to marine), and *Anthraconaia-Cyzicus* (shoreline, fresh to brackish water). The coastal/deltaic plain facies contains terrestrial plant bearing coaly intervals (Grenda, 1977) overlying well-developed paleosols (Barwis, 1990), freshwater limestone, and red beds. Even though all three depositional environments may be present within a given vertical section, the prevalence of deeper water marine facies are found near the center of the basin whereas terrestrial facies dominate the upper reaches of the basin flank to the south and east. A transitional facies between the marine and terrestrially dominated facies associations contains the conventional sandstone reservoirs in the Tyler producing fields situated along the east-west trending Dickinson-Fryburg trend.
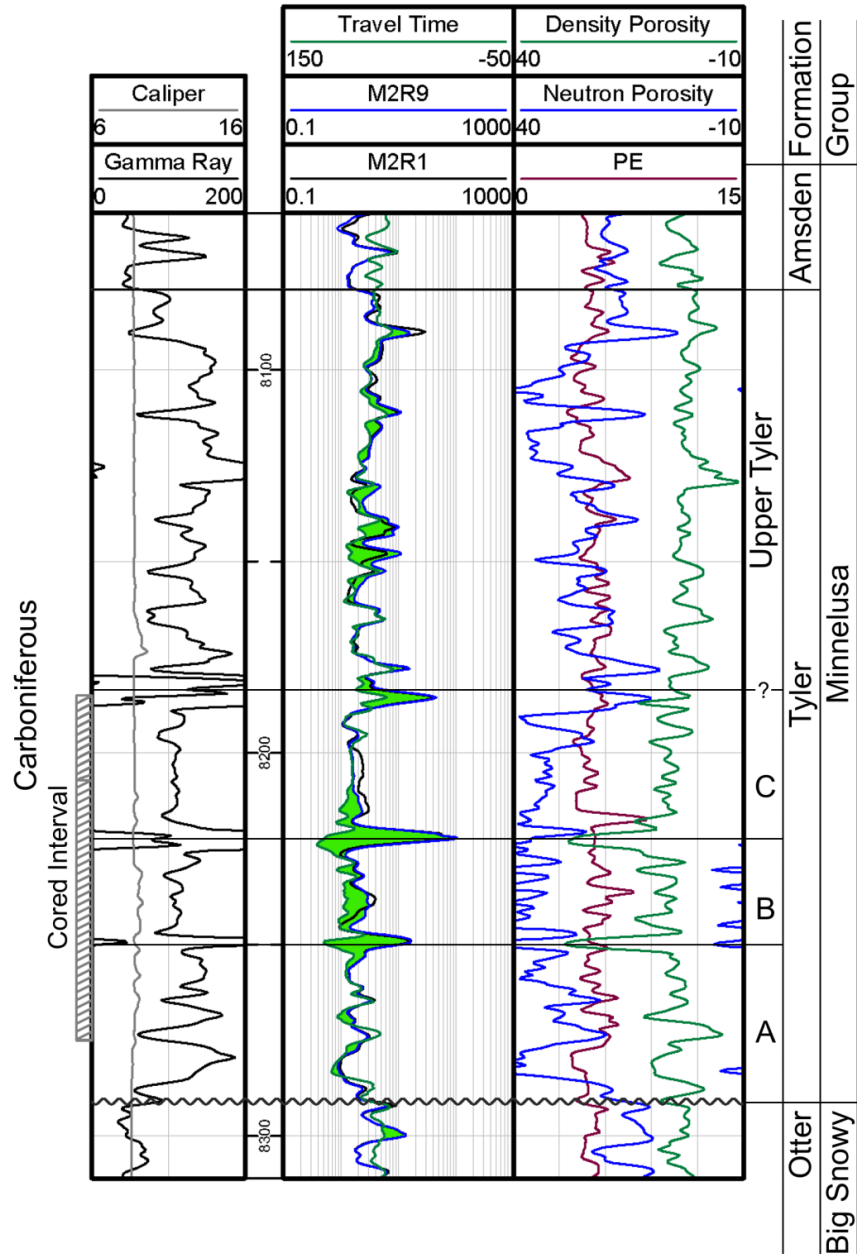
Figure 1.1. Representative wire line log of the Tyler Formation showing three "cycles" of the central basin facies. The green shaded areas on the transit time and resistivity track (M2R9, M2R1) represent log derived organic carbon estimates using the Passey (1990) method.
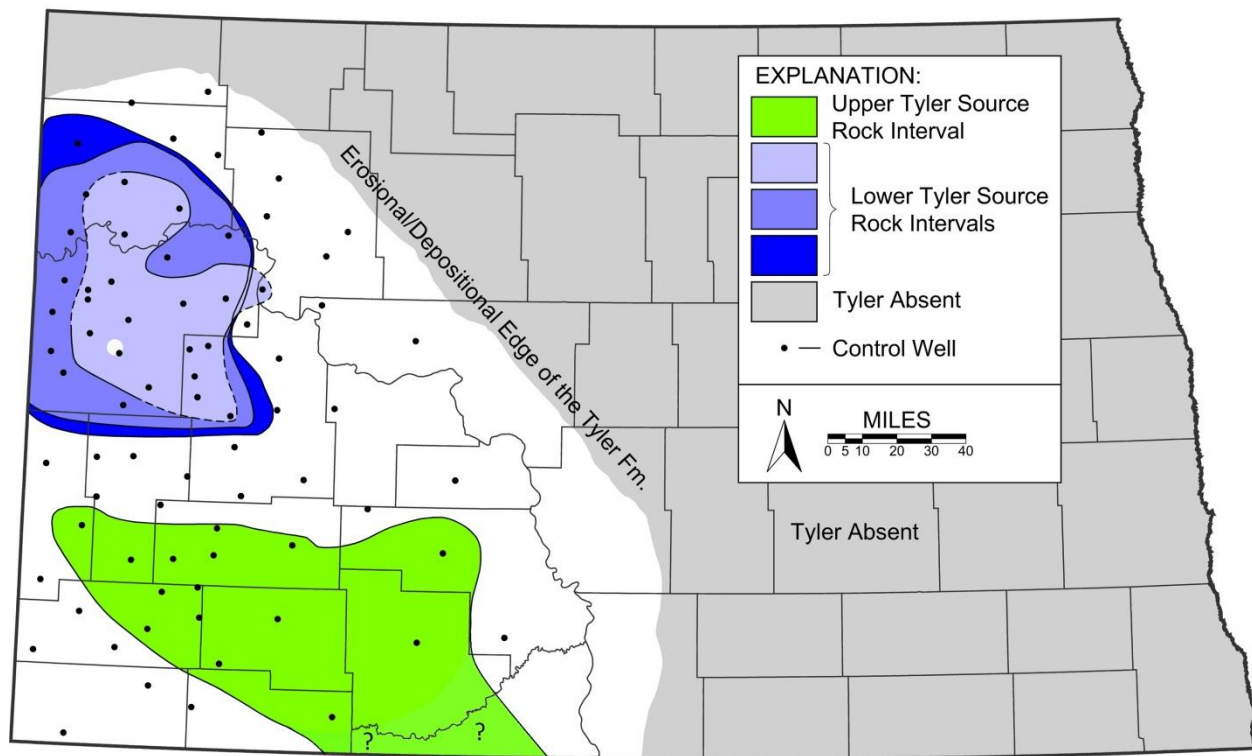
Fig. 1.2. Generalized map of the distribution of potential source rocks in the Tyler Formation. The portions of the map in shades of blue are found in the lower portion of the Tyler whereas the area in green represents the distribution of potential source rocks in the upper part of the formation.

Organic Content

The total organic carbon (TOC) content of source rocks is of first order importance in the evaluation of a petroleum systems oil generation potential. In this study the weight percent TOC was obtained from 842 cuttings samples from 54 wells and 25 core samples from another 5 wells. Weatherford Labs analyzed these samples using the LECO TOC method. An additional 82 older TOC analyses from cores of two additional wells are on file with the NDGS and are included in this study.

The frequency distribution of the TOC analyses is positively skewed and has an average of 1.81% with a variance of 16.4 (Fig. 1.4).
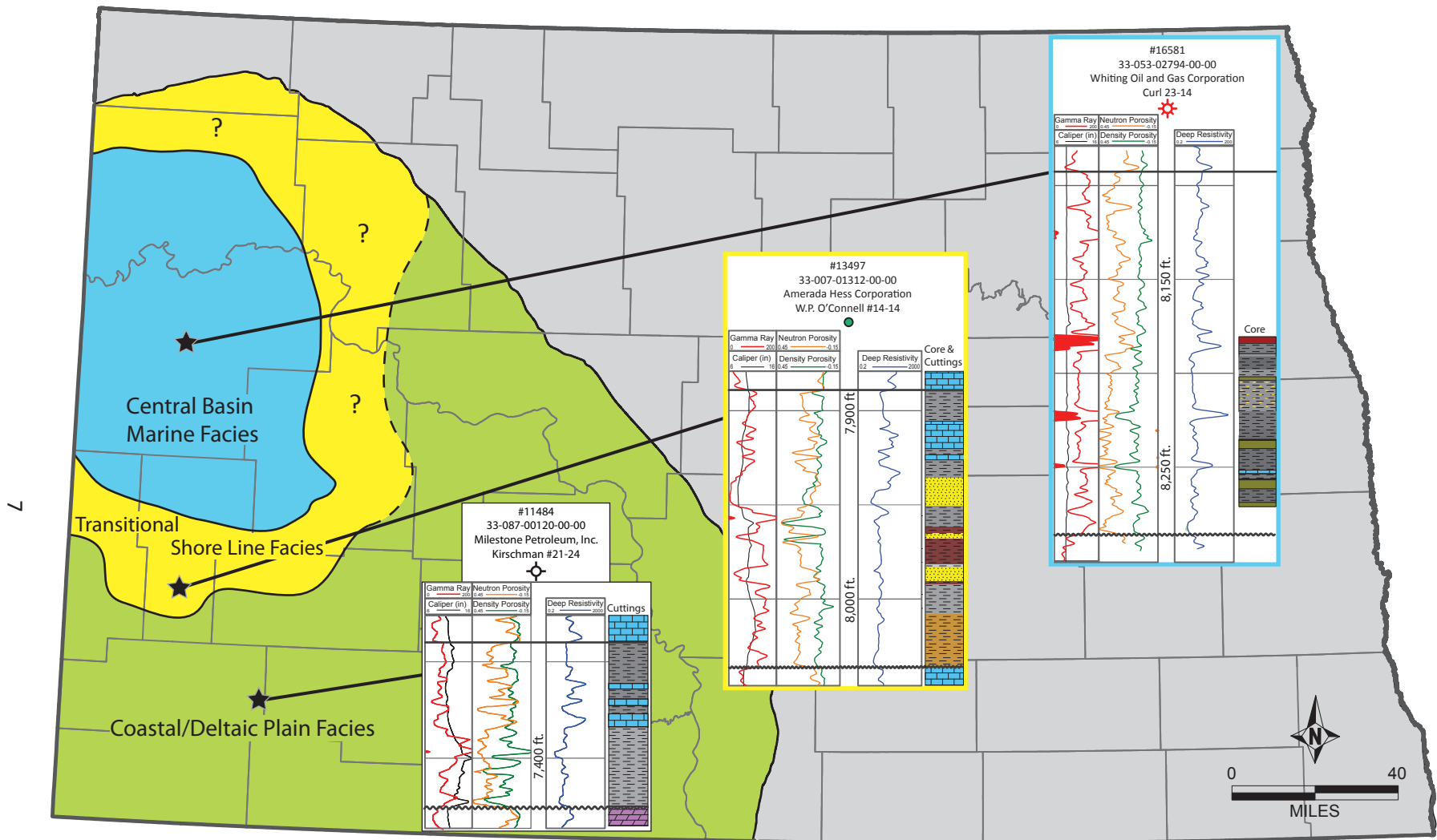
Figure 1.3. Schematic map of the regional facies tracts present in the Tyler Formation of North Dakota. The grey portions of the map represent areas in which the Tyler Formation is absent (after Anderson, 1974).
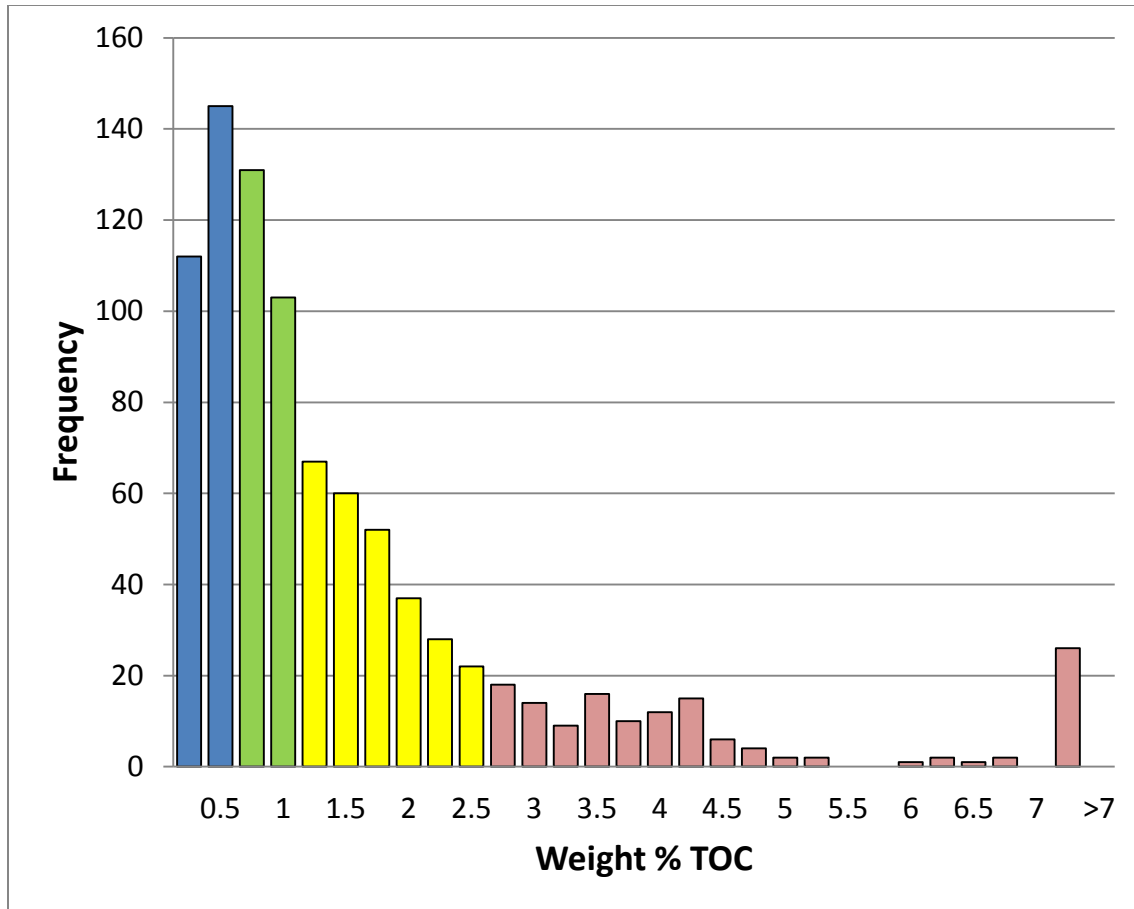
Figure 1.4. Frequency distribution of weight % total organic carbon found in samples of cuttings and cores from the Tyler Formation in North Dakota. The data represented in blue correspond to samples containing poor amounts of TOC. Sample containing "fair", "good" or "excellent" amounts of organic carbon are shown in shades of green, yellow and pink respectively. The classification is based on the system used by Dembicki (2009).

The average regional distribution of total organic content in the Tyler Formation is shown in Fig. 1.5. The contours are drawn using the average TOC measured in the samples and core for each well shown. This map illustrates a rough correspondence with the three depositional facies tracts described earlier.
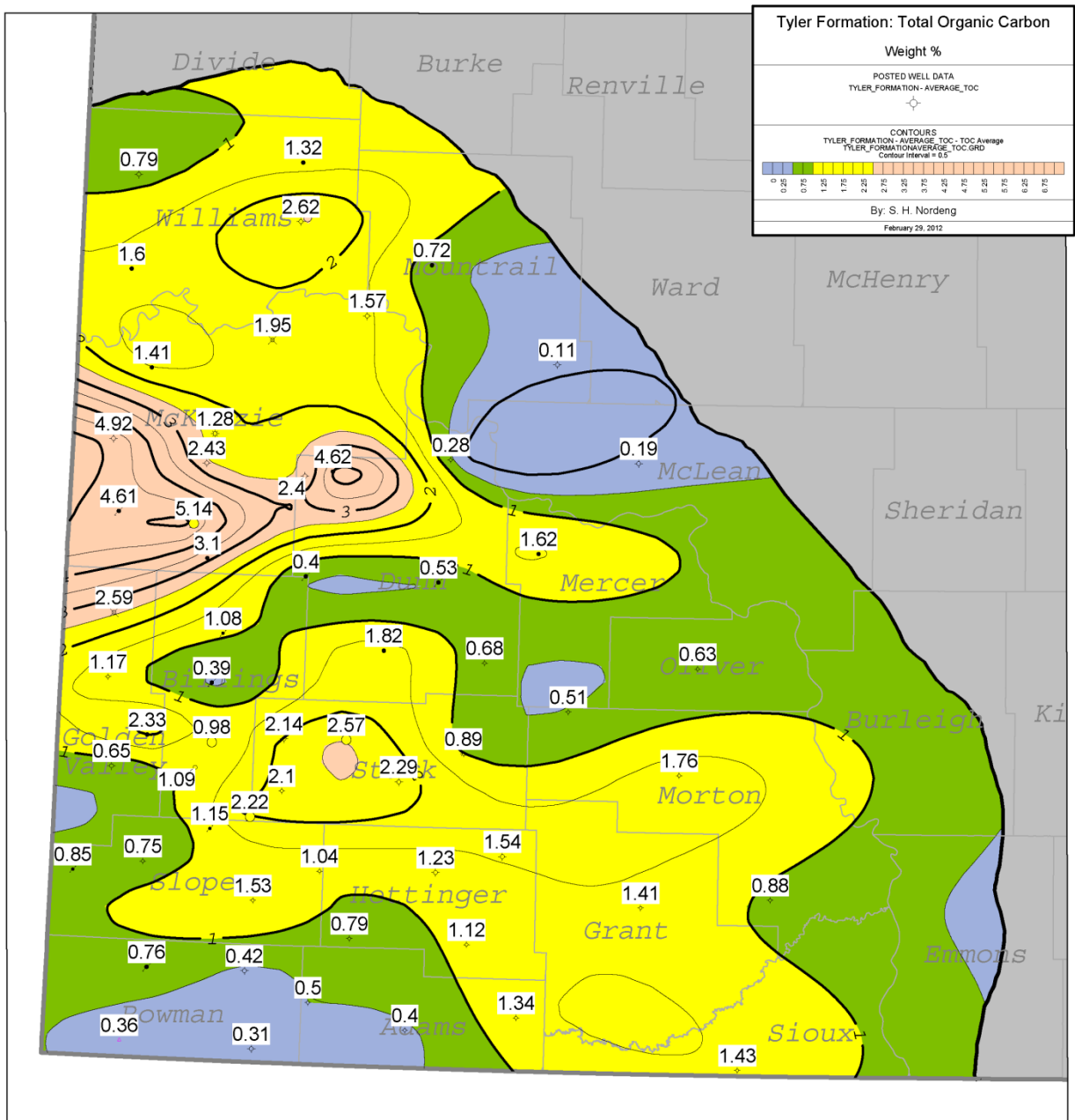
Figure 1.5. Map showing the average TOC content of the Tyler Formation in the western half of North Dakota. The color scheme is keyed to the classification used by Dembicki (2009) where "fair", "good" or "excellent" amounts of organic carbon are shown in shades of green, yellow and pink respectively. The Tyler Formation is absent in the portion of the map in gray (Anderson, 1974).

Kerogen Type

TOC analysis, though important, does not provide any information as to the type of petroleum that might be expected to form upon maturation. The products generated during the maturation of a given kerogen are related to the amount of hydrogen bonded carbon and oxygen bonded carbon that is

present. Kerogen that is very rich in hydrogen bonded carbon tends to generate oil whereas kerogen that has smaller amounts of hydrogen bonded carbon and larger amounts of oxygen bonded carbon tend to produce gas. Kerogen with oxygen and hydrogen contents that lie between these extremes tend to produce both oil and gas.

 Rock-Eval pyrolysis may be used to estimate the amount of hydrogen bonded carbon and oxygen bonded carbon that is present in a sample. These two measures of organic composition form the basis for predicting what types of petroleum could be expected to form during thermal maturation of a given kerogen.

This is usually done by cross-plotting the hydrogen index (HI) against the oxygen index (OI). The hydrogen index (HI) is the mass of hydrogen-bonded carbon contained in a sample normalized to the samples total organic content (Eq. 1.1). The oxygen index is a normalized measure of the oxygen bearing organic compounds (Eq. 1.2). One popular kerogen classification method plots Hydrogen Index against the Oxygen Index on a modified Van Krevelen diagram. The modified Van Krevelen diagram includes type curves that trace the HI and OI trends that correspond with four broad kerogen types (Dembicki, H., 2009). Application of this method to data collected for the Tyler Formation is presented in Fig. 1.6 and Fig. 1.7.

Eq. 1.1 $$HI = (S_{2\ (mg\ HC/g\ sample)}/TOC)*100$$

Eq. 1.2 $$OI = (S_{3\ (mg\ CO2/g\ sample)}/TOC)*100$$

The interpretation of modified Van Krevelan diagrams requires care. This is because during oil generation the kerogen bound hydrogen is lost to the newly formed petroleum products. Rock eval analysis of samples that have undergone some level of oil generation will yield lower HI's than were originally present.
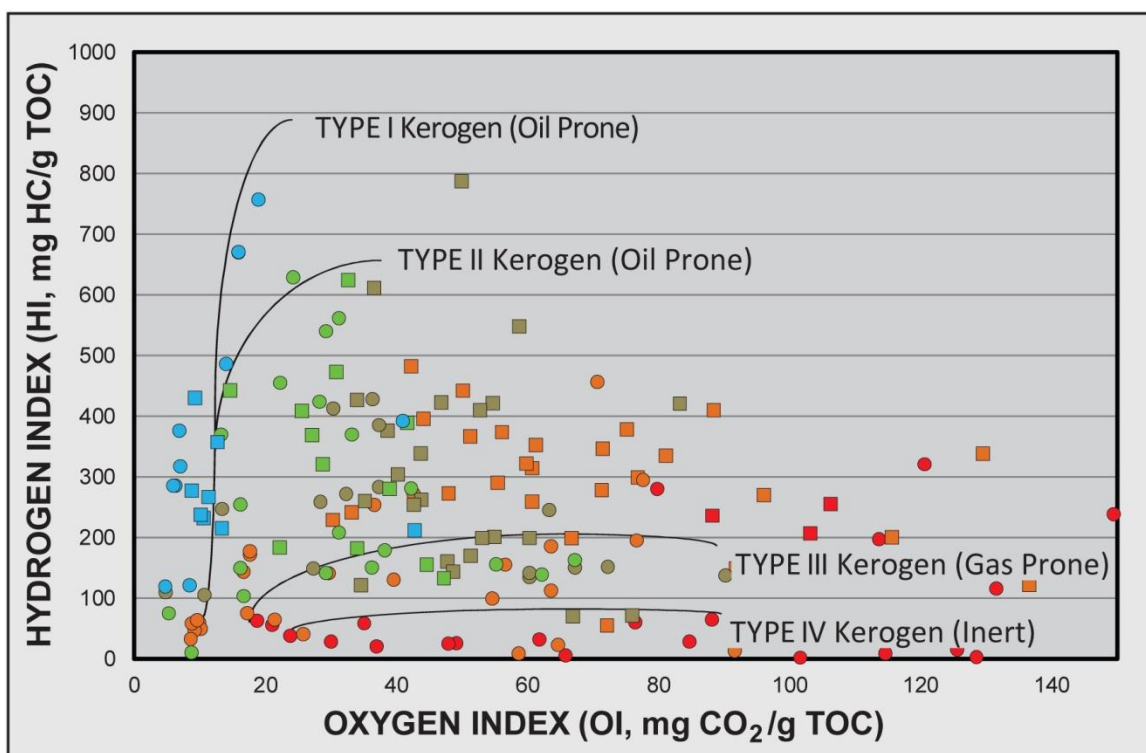
Figure 1.6. A modified Van Krevelen diagram with the composite Tyler RockEval data set, which plots Hydrogen Index (HI) versus Oxygen Index (OI) to determine the type/s of kerogen present. Type I and II kerogen are prone to generate oil while type III kerogen is prone to generate gas. Type IV kerogen is inert, and is not prone to generate oil or gas. Square data points represent cutting samples and circles represent core samples. The color scheme follows that of Figure 1.7.

The hydrogen and oxygen indices, when plotted on a modified van Krevelan diagram (Fig. 1.6), do not indicate the presence of a single kerogen type in the Tyler Formation. This is not surprising given that the depositional cyclicity resulted in thin packages of lithofacies that include off-shore marine and on-shore terrestrial environments all within a vertical section that frequently is less than ten feet thick. However, separating the samples on the basis of TOC does show a systematic trend in kerogen type. Specifically, samples containing more than five percent TOC plot closely to the Type I – Type II curves (Fig. 1.7A). Samples containing between one and two percent TOC show a tendency to cluster about the Type III curve (Fig. 1.7D) while samples containing less than one percent TOC generally plot between the Type III and Type IV curves (Fig. 1.7E). One might speculate that the data scatter represents a mixing of lithofacies during drilling and sample collection. However, close examination of the data does not reveal any apparent difference in the results from cuttings containing a mixture of lithofacies and samples of single lithofacies collected from core. This lack of distinction suggests that the end member kerogen types were probably mixed during deposition.
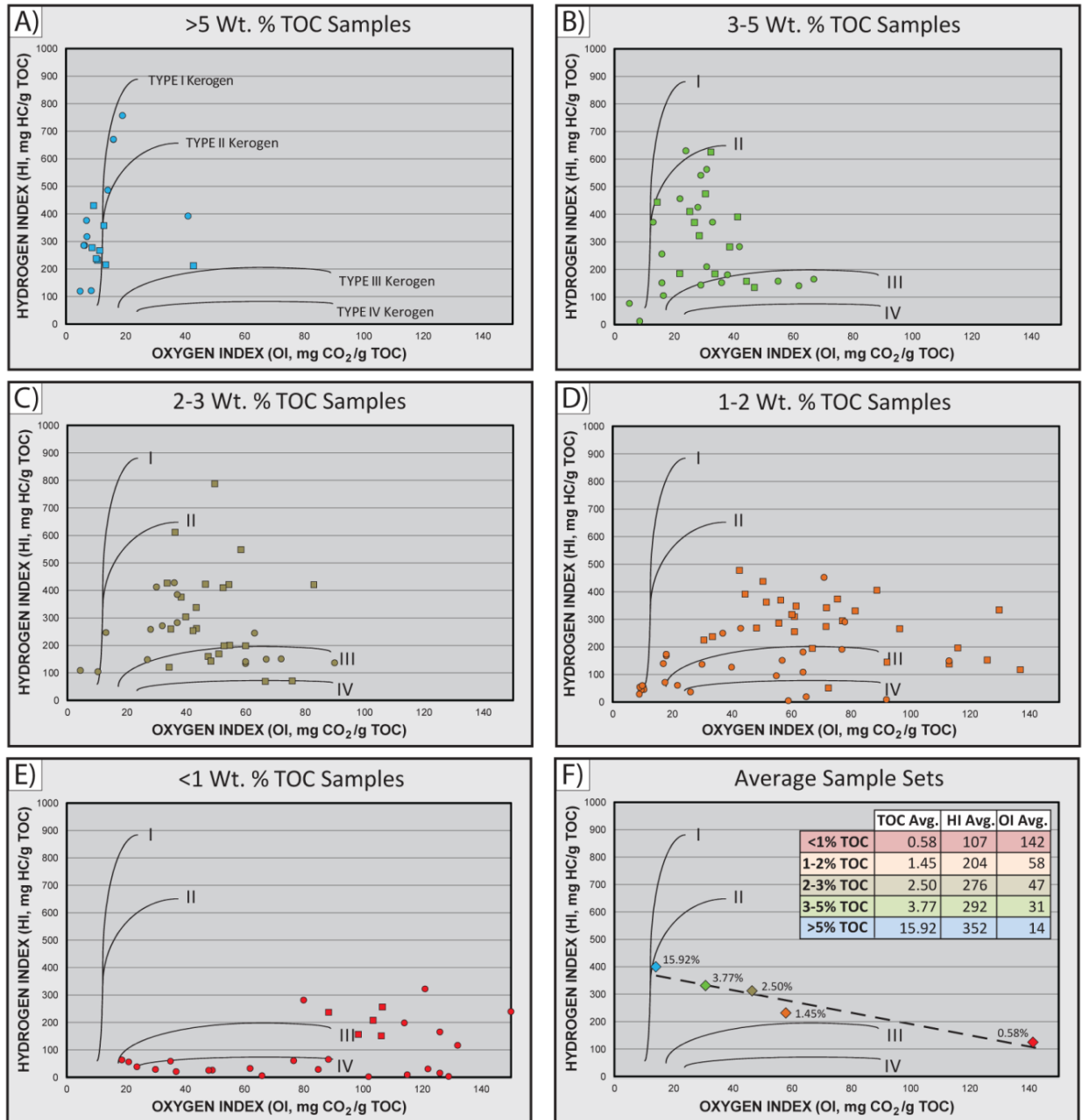
Figure 1.7. Modified Van Krevelen diagrams characterizing the kerogen type of analyzed Tyler samples based on TOC content. 1.7a) Samples with greater than 5 wt. % TOC contain primarily type I/type II kerogen. 1.7b-f) As TOC content declines, the kerogen type transitions to type III and type IV.

Plotting the average value of the OI and HI for each of the classes presented in Fig. 1.7 shows an almost linear trend of decreasing HI with increasing OI as the average TOC content decreases (Fig. 1.7F). This diagram suggests that samples with higher TOC content are more likely to generate oil (Type I - Type II) whereas samples with lower TOC content are more likely to generate gas (Type III) or be inert (Type IV).

Organic Richness

The determination of the TOC content or kerogen type is usually insufficient to gauge the quality and richness of a source rock. This is because the measure of TOC includes both "live" and "dead" or inert kerogen (Type IV). The TOC that is "live" may be prone to generating only gas (Type III), only oil (Type I) or some mixture of oil and gas (Type II) (Jarvie, 1991). The difference between "live" and "dead" kerogen is that "live" kerogen is capable of generating hydrocarbons whereas "dead" kerogen is not. The tendency of a given kerogen to generate oil, gas or some combination of the two depends a great deal on the distribution of organic compounds present in the "live" kerogen. Kerogen that has a large proportion of constituent compounds containing hydrogen tend to generate oil whereas compounds with less hydrogen and more oxygen tend towards gas generation. The relative contribution of organic hydrogen to the total kerogen composition together with the TOC content is one way in which the organic richness of a kerogen may be assessed. Rock-Eval pyrolysis provide useful data that address this issue (see Nordeng, 2012 for details and additional references). Specifically, the total mass of hydrocarbons evolved during the programmed pyrolysis is a direct measure of the hydrocarbon content of a source rock. A plot of the evolved hydrocarbon mass versus the TOC provides a semi-quantitative estimate of kerogen richness. Fig. 1.8 shows that a significant number of samples from the Tyler Formation contain "good" to "excellent" quantities of both TOC and hydrocarbon generating kerogen (S_2). These "rich" organic source beds could be expected to generate significant amounts of hydrocarbons given sufficient temperatures to drive hydrocarbon generation. However, in order to properly evaluate the data it is important to remember that during maturation, source rocks become depleted in both hydrocarbon generating kerogen (S_2) and TOC. Therefore, samples classified as being only "fair" may have been much richer prior to hydrocarbon generation (Dembicki, 2009).

Results of the Rock-Eval and TOC analyses of the Tyler Formation suggest that the richest source rocks are associated with black radioactive shale found in the central basin facies. These rocks have the highest TOC and HI and would therefore be likely to generate oil and gas when sufficiently mature.
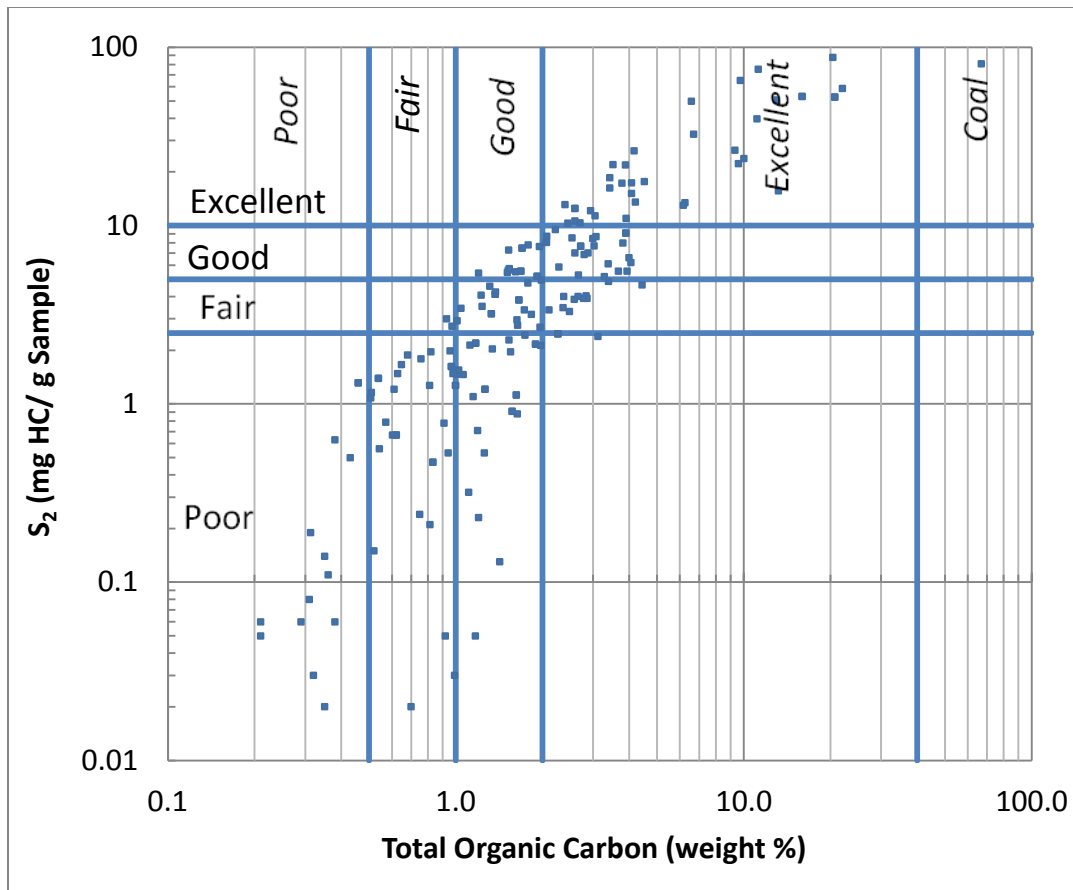
Figure 1.8. A plot of the total mass of hydrocarbons derived by thermal decomposition of kerogen (S₂) versus the TOC content of cuttings and core samples of the Tyler Formation.

2) Maturation

Based on the similarities in unique (to the Williston Basin) paraffin content between oils produced from the Tyler Formation and those found in the source beds within the Tyler Formation, Dow (1974) and Williams (1974) concluded that the oil within the Tyler Formation was locally derived. The question as to the level of maturity that the kerogen in the Tyler Formation has achieved is largely a problem that involves the rate at which chemical reactions occur as kerogen converts to oil. These chemical reactions are critically dependent upon the temperature history and reactivity of the kerogen in question. This study employs a dual approach to addressing this issue. The first approach is essentially a theoretical exercise that makes use of a simple model of kerogen conversion rates as a function of burial induced temperature changes. Essentially the method attempts to reconstruct the burial history of the Tyler Formation and from this model reconstruct the temperature and kerogen reaction history. The second approach uses the results from Rock-Eval programmed pyrolysis experiments. These data are frequently used to evaluate the level of maturation within a given source rock. However, neither method alone is capable of establishing the level of maturity of a source rock unequivocally. Therefore, the goal is to use

the two approaches together to estimate the level of thermal maturity present in the Tyler Formation. A third method that is indirectly related to the issue of source rock maturation makes use of electric logs that are commonly employed to evaluate formations for the presence of oil. This method makes use of the idea that as kerogen within a source rock converts to petroleum, the original electrically conductive water is replaced by nonconductive oil or gas. This change in the formation fluids electrical behavior is evident on logs that measure the electrical resistivity of the borehole environment.

Thermal History of the Tyler Formation

Methods

The thermal history of a subsurface unit is a combined function of the heat that flows through a stratigraphic section, the long-term surface temperature and thermal characteristics of the various lithologies present in the section. These factors are frequently described in terms of Fouriers's law of heat conduction. Fourier's law describes how temperature changes (ΔT) when heat flows at a constant rate (Q) through some thickness (L) of material that has a constant thermal conductivity (K). For a single layer, the following expression holds:

Eq. 2.1 $\Delta T = Q\,L/K$

In order to estimate the temperature at the base of a stack of material, Eq. 2.1 must be expanded to include the temperature change caused by the various thermal conductivities and thickness of each layer. Estimates of the temperature at depth (T_n) are found by adding the temperature changes (QL_i/K_i) associated with each deeper stratigraphic unit (i=1…n) to the "mean" surface temperature (T_o) as follows (Blackwell and Richards, 2004):

Eq. 2.2 $T_n = T_o + Q(\,L_1/\,K_1 + L_2/\,K_2 + \ldots + L_n/\,K_n)$

Where:

       n is the number of stratigraphic units in the section where i=1…n
       T_n is the temperature at the base of the nth unit (^{o}C)
       T_o is the average surface temperature (^{o}C)
       Q is the conductive heat flow (mW/m^2)
       L_i is the thickness of the ith unit (m)
       K_i is the thermal conductivity of the ith layer (W/m-^{o}K)

Estimating a given formation temperature using Fourier's law requires that the thermal conductivity of each layer together with the conductive heat flow and average surface temperature be known. These can be found by plotting subsurface temperature against depth. If the temperatures measured are from a section that contains a single thermal conductivity then Fourier's law predicts that the temperature gradient will be linear with depth.

15

The slope of the temperature gradient is a function of the thermal conductivity of the formation and conductive heat flow. Under steady state, constant heat flow, the slope of the temperature gradient is proportional to the thermal conductivity. Thermally conductive formations have steeper thermal gradients (degrees per foot or meter) than do thermally less conductive formations with the difference in the temperature gradient being proportional to the difference in thermal conductivity. Therefore, if one knows or assumes a conductive heat flow then it is possible to find a set of thermal conductivities that will fit an observed temperature profile. This can be done by subdividing the section into thermal units that exhibit a constant (linear) change in temperature with depth. Segments of a stratigraphic section that exhibit a linear gradient may be assumed to have a constant thermal conductivity. Thermal conductivities may be determined experimentally under laboratory conditions using known heat flows. However, in the absence of experimental results, estimates of thermal conductivity may be made from temperature-depth measurements when the geothermal heat flow is known. Rearranging Eq. 2.1 and using linear regression to find the temperature gradient for the selected stratigraphic intervals in Table 2.1 results in a solution for thermal conductivity:

Eq. 2.3 $\qquad K = Q\, L\, /\, \Delta T$

Where:

K = the thermal conductivity (W/m-^{o}K)
$\Delta T/L$ = the thermal gradient (^{o}C/m)
Q = geothermal heat flow (W/m^2).

In this study, a temperature log from the Rauch Shapiro Fee #21-9 was used to find the thermal conductivities of the units above the Tyler Formation. The temperature log also provides an estimate of an "average" or "long-term" surface temperature.

The Rauch Shapiro Fee #21-9, spudded on June 11, 1980, reached a total depth of 12,741' on September 7, 1980. Problems with cementation of the production string resulted in additional operations that ended prior to running a cement bond (CBL) and temperature logs on November 2, 1980. The well initially completed in the Bakken and Three Forks formations produced 264 barrels of oil. The well was subsequently converted into a salt water disposal well and was plugged and abandoned in August 2008. Even though the timing of the various cementing operations are not well known, the total depth for which temperature readings are available make this well an attractive subject for the determination of the thermal conductivities for most of the section present in the Williston Basin.

In order to use Fourier's law in this situation, an estimate of the geothermal heat flow must be made. This was done for the Rauch Shapiro #21-9 by interpolation of Blackwell and Richard's (2004) heat flow map (Fig. 2.1). Based on this map, the heat flow in the Rauch Shapiro Fee #21-9 is estimated to be 65.1 mW/m^2. Using this heat flow value and the temperature gradients from the temperature log, the thermal conductivities listed in Table 2.1 were found with Eq. 2.3. For example, if the temperature

gradient (ΔT/L) through the Tyler Formation is 0.0214°C/m and the geothermal heat flow (Q) is 0.06512 W/m^2 , then solving Eq. 3 yields a thermal conductivity for the Tyler Formation of 3.0 (W/m-°K).

In order to use Eq. 2.2 to estimate subsurface temperatures, the average surface temperature must also be known. In many instances average surface temperatures are obtained from weather records. However, these records are of short geological duration and may not be a true representation of a geologically meaningful average temperature (Gosnold, pers. com.). A more meaningful average surface temperature might be obtained by extrapolating the shallow subsurface temperature gradient (>300 feet or 100 m) to the surface. The relatively shallow temperature profile (<1,500 m) within the Rauch Shapiro is remarkably linear throughout the Pierre Formation, the shallowest formation for which temperature data is available. Extrapolation of this temperature data to the surface (see Figure 2.2) suggests that the long-term average surface temperature is about 17.45°C. Using this as the surface temperature in Eq. 2.2 and the thermal conductivities in Table 2.1 results in a modeled thermal profile (yellow squares; Figure 2.2) that corresponds well with the entire measured temperature profile.
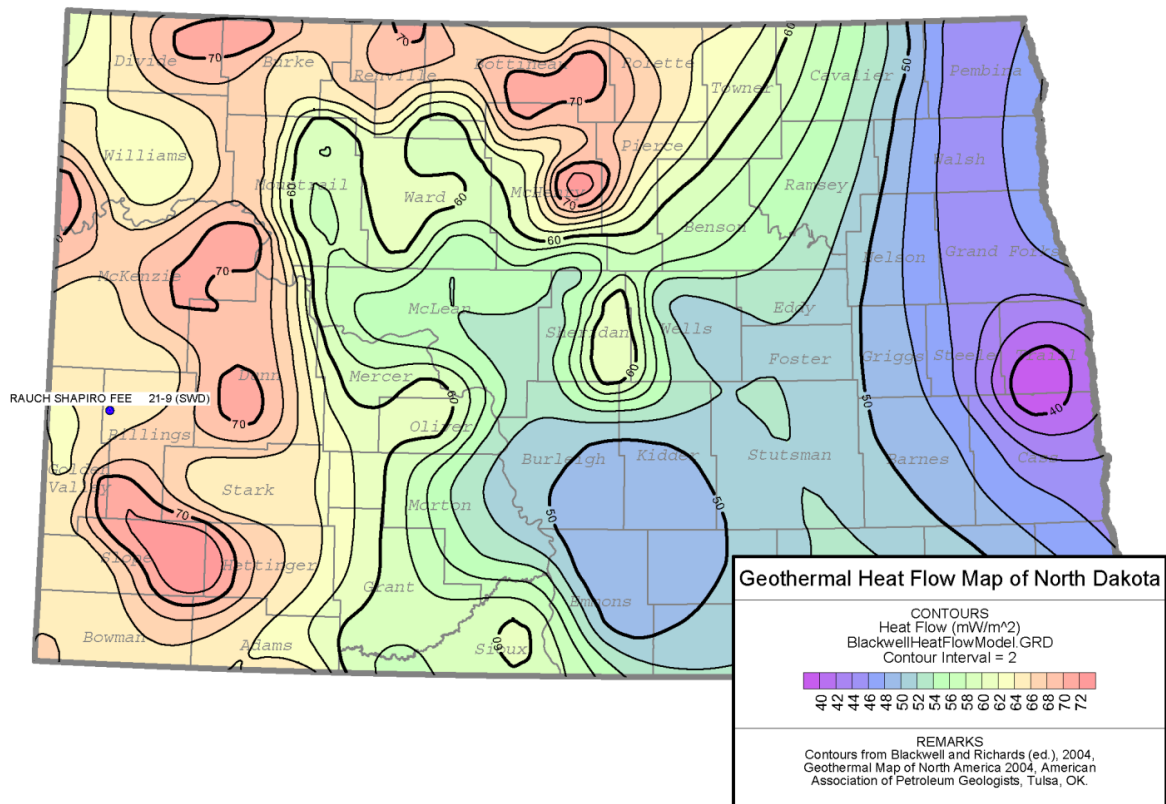
Figure 2.1. Heat flow map of North Dakota (from Blackwell and Richards (2004) with the location of the Rauch Shapiro Fee 29-1 drilled by Diamond Shamrock Corp. in the NE ¼, NW ¼, Sec. 9, T142N, R102W of Billings County, North Dakota.
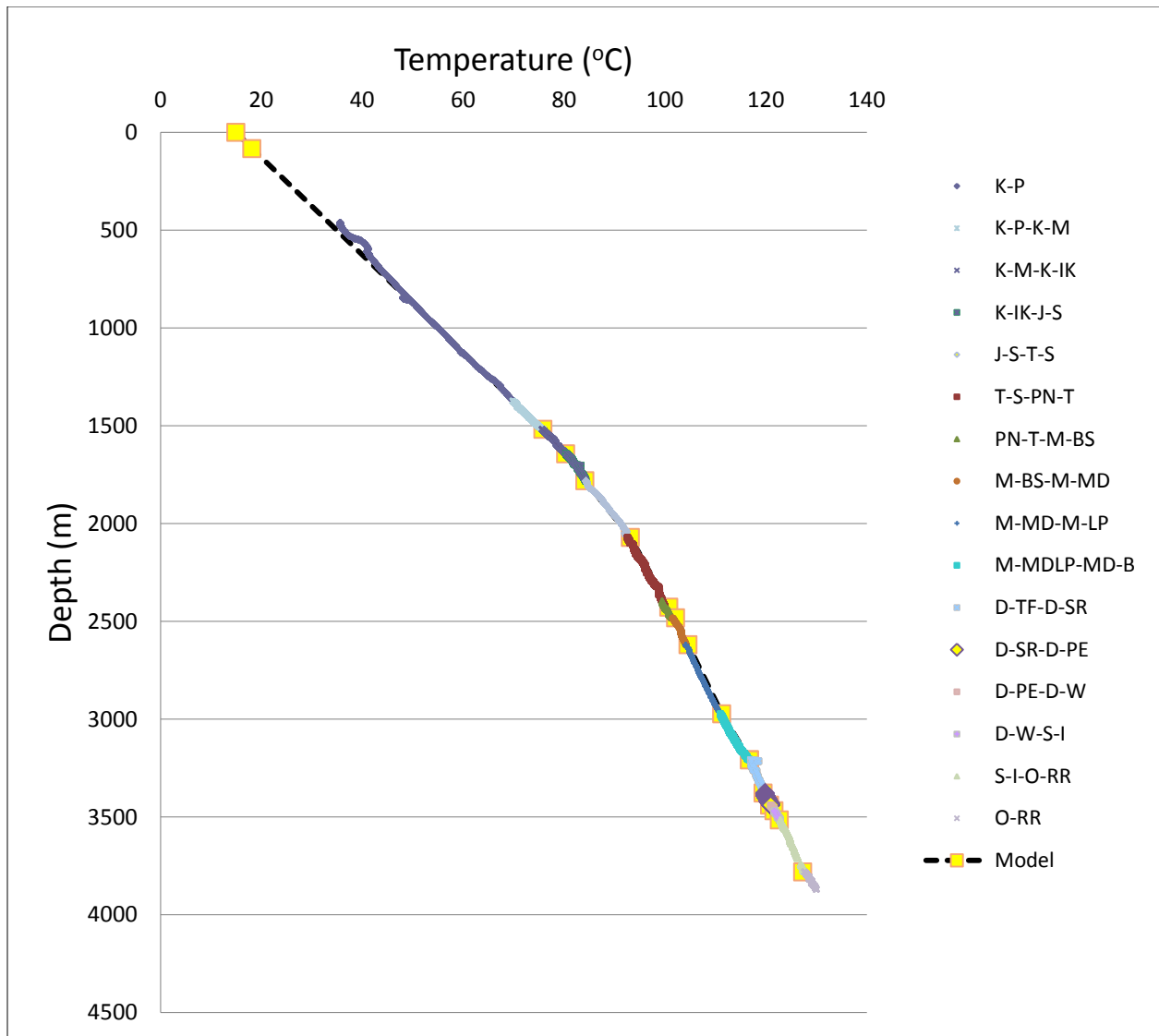
Figure 2.2. Temperature-Depth profile for the Rauch Shapiro Fee #29-1. The "average" surface temperature, found by extrapolating the temperature-depth trend defined by the section above the Mowry Formation, is 17.45 $^{\circ}$C (R^2 = 0.997). Use the unit code column in Table 2.1 as a reference to the formation tops that define the thermal stratigraphy used above.

Table 2.1. Thermal conductivities of units present in the Rauch Shapiro Fee #21-9 (API#: 33-007-00526-00-00) based on a constant conductive heat flow of 65.12 (mW/m^2) .

Unit	Unit Code	Depth (ft)	Depth (m)	Thermal Gradient (°C/m)	Intercept (°C)	R^2	Thermal Conductivity (W/m-°K)
Surface		0	0				
Sentinel Butte		-202	-61.570				1.72*
Pierre	K-P	1733	83.184	0.0379	17.446	0.9974	1.72
Mowry	K-M	4980	1517.904	0.0402	14.573	0.9128	1.62
Inyan Kara	K-IK	5393	1643.786	0.0362	20.836	0.8469	1.80
Swift	J-S	5844	1781.251	0.0277	35.122	0.969	2.35
Spearfish	T-S	6794	2070.811	0.031	29.183	0.9901	2.10
Tyler	PN-T	7963	2427.122	0.0214	48.41	0.9915	3.04
Big Snowy	M-BS	8146	2482.901	0.0243	41.07	0.98	2.68
Madison	M-MD	8596	2620.061	0.018	57.06	0.967	3.62
Lodgepole	M-LP	9755	2973.324	0.0189	54.71	0.9986	3.45
Bakken	MD-B	10521	3206.801	0.0235	40.842	0.994	2.77
Three Forks	D-TF	10526	3208.325	Bakken too thin			2.50**
Souris River	D-SR	11083	3378.098	0.0157	66.835	0.8924	4.15
Prairie Evap.	D-PE	11284	3439.363	0.0211	48.489	0.9877	3.09
Winnipegosis	D-W	11380	3468.624	0.0299	18.177	0.9834	2.18
Interlake	S-I	11534	3515.563	0.023	41.862	0.979	2.83
Red River	O-RR	12403	3780.434	0.0175	61.473	0.9938	3.72
TD		12762	3889.858	0.0255	31.45	0.9886	2.55

*Assumed thermal conductivity based on linear relationship with underlying Pierre Fm.
** Plausible shale value.

Determination of Maturity of the Tyler Formation in the Rauch Shapiro Fee 21-9

Estimating the thermal maturity of the Tyler Formation requires knowledge of the thermal history of the formation. This is done by reconstructing the burial history and, with the information present in Table 2.1, a reconstruction of the formation's temperature history. The temperature history can be used to estimate, at least from a theoretical standpoint, the level of thermal maturity that organic matter within the Tyler has achieved. Wood (1988) presents a method that expresses a source rock's level of organic maturity in terms of the amount of kerogen that has been converted to petroleum. Wood does this with the Arrhenius equation (Eq. 2.4) in which the rate of petroleum generation is linked to temperature and parameters that describe the kinetics of the kerogen involved.

Eq. 2.4 $$k = A\, e^{-Ea/RT}$$

Where:

k = reaction rate (mol/m.y)
A = Frequency at which potential reaction states or collisions occur (1/m.y)
E_a = Activation energy (kJ)
R = Gas constant (0.008314 kJ/mol-^{o}K)
T = Temperature (^{o}K)

Wood's method requires several assumptions. These include estimates of the activation energy (E_a) and frequency factor (A) that define the reaction rate in Eq. 2.4. The value of E_a and A used in this study was experimentally determined.

Experimental Determination of E_a and A

The activation energy and corresponding frequency factor are fundamental parameters that describe the rate at which kerogen decomposes into petroleum products. A single sample was collected from a core of the Tyler Formation that was taken by the Atlantic Richfield Company while drilling the Harmon 1-26 (API: 33105011220000; NDIC: 10931) in Section 26, T. 156, N. R. 100 W., Williams County, North Dakota. The well, drilled as a vertical test to a total depth of 10,043' M.D., was completed in the Madison Formation with a reported I.P. of 233 bbls/D. The top of the Tyler Formation was encountered at a depth of 7,685'M.D.. Two sixty-foot cores were taken from in the Tyler Formation between the depths of 7,743' to 7,863' M.D.. The sample used in this study is a dark gray to black shale taken from core at a depth of 7,803.5' M. D. (Figure 2.3). This interval was selected because it: 1) contained the high gamma ray response that is a characteristic signature of the central basin marine facies and 2) the well appeared, on the basis of Rock Eval T_{max} and depth, to be the least mature example of this stratigraphic interval that had a core on file with the North Dakota Geological Survey.

Figure 2.3. Photograph of the core from which the sample used to find the activation energy and frequency factor was taken.

The sample collected from the Harmon 1-26 was submitted to Weatherford Laboratories for analysis. The analysis used a Rock Eval 6 instrument and involved a programmed pyrolysis scheme using five heating rates (2, 5, 10, 25 and 50 °C/min). The raw data consist of the fraction of evolved hydrocarbons relative to the maximum amount detected and the corresponding temperature (see Figure 2.4)
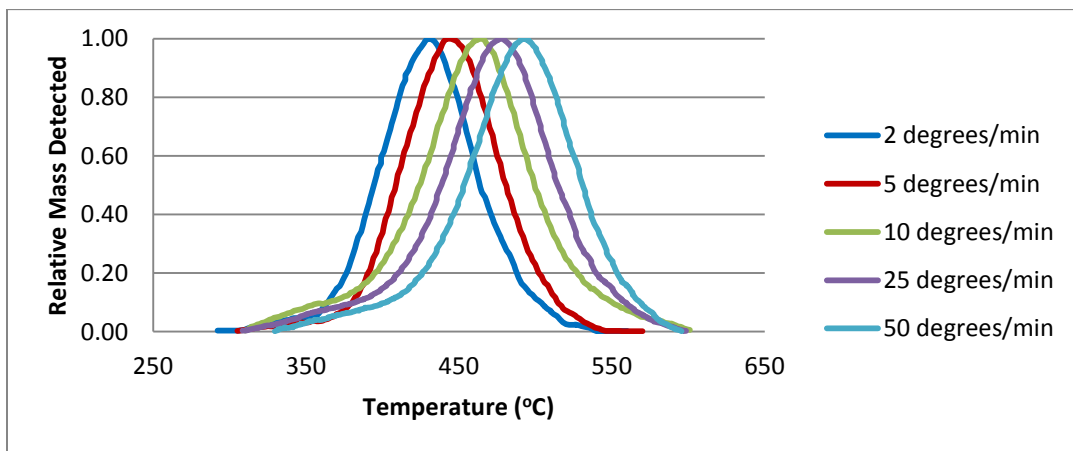
Figure 2.4. Pyrograms obtained from Rock Eval 6 analysis with the Y-axis scaled to the maximum mass recorded. This maximum mass defines the value of T_p for a particular heating rate. The values of T_p for each heating rate are in Table 2.1.

The method employed is based on the Kissinger method in which the rate of kerogen decomposition is assumed to be a first order reaction that obeys the Arrhenius equation with respect to temperature as follows:

Eq. 2.5
$$d\alpha/dt = A \exp(-E_a/RT)(1-\alpha)$$

Where:

$d\alpha/dt$ = transformation rate
α = fraction of kerogen converted
t = time (min)
A = Frequency factor (min^{-1})
E_a = activation energy (kJ/mole)
R = gas constant (kJ/mole-^{o}K)
T = Temperature (^{o}K)

Kissinger (1957) provides an approximate solution to Eq. 2.5 for reactions that take place while temperatures increase at a constant rate. His solution provides the following relationship that uses the the temperature that corresponds with the maximum rate of conversion (T_p) from multiple experiments in which the heating rate (β) is varied (Kissinger, 1957):

Eq. 2.6
$$\ln(\beta/T_p^2) = \ln(A R/E_a) - E_a/RT_p$$

Where:

β = heating rate (^{o}C/min)
E_a = Activation Energy (kJ/mole)
R = .008314 kJ/mole-^{o}K
A = Frequency Factor (min$^-$)
T_p = Temperature that corresponds with maximum hydrocarbon generation (^{o}K)

Equation 2.6 finds the activation energy (E_a) and frequency factor (A) from a plot of the $\ln(\beta/T_p^2)$ versus $1/T_p$. A straight-line data plot should have a slope equal to E_a/R and an intercept equal to the Ln (A R/E_a). Regression analysis of the data in Table 2.2 that (Fig. 2.5) finds that the best-fit line has a slope of 26,075 ^{o}K and an intercept of -24.64 ^{o}K/min with an R^2 of 0.989. The slope, when multiplied by the gas constant 0.008314 kJ/M-^{o}K), results in an activation energy of 217 kJ/mole. Inserting the slope into the expression for the intercept (-24.64 = -ln (A R/E_a)) and solving it for A results in a frequency factor of 1.306 X 10^{15} min^{-1} or 6.86 X 10^{26} m.y.$^{-1}$.

$T_p(°C)$	$T_p(°K)$	Heating Rateβ (°C/min)	$Ln(T_p^2/\beta)$	$1/T_p(°K)$
431	704.15	1.998	12.42183612	0.00142
444	717.15	4.992	11.54273342	0.001394
465	738.15	9.966	10.90911481	0.001355
477.5	750.65	24.798	10.03111599	0.001332
492.5	765.65	49.332	9.382877335	0.001306

Table 2.2. T_p and measured temperature data used to find the activation energy (E_a) and frequency factor (A). The data are from a sample of core taken from the Harmon 1-26 (NDIC # 10931) at a depth of 7,803.5 feet M.D.
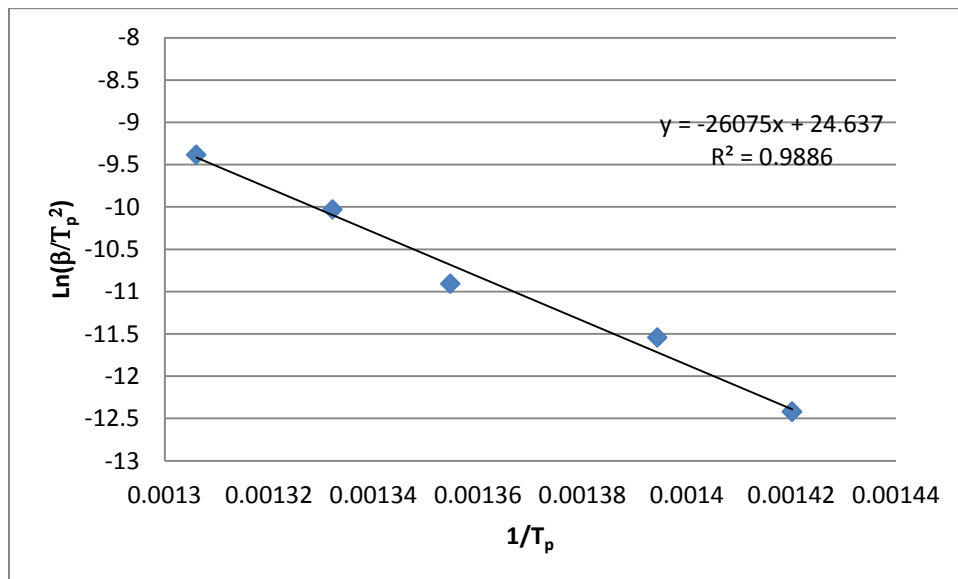
Figure 2.5. Kissinger plot for the data in Table 2.1 used to find the activation energy and frequency factor for the sample from the Harmon 1-26 (NDIC # 10931). β is the heating rate (°C/min) and T_p is the temperature (°K) that corresponds with the maximum rate of hydrocarbon generation.

The kinetic parameters obtained from the Harmon 1-26 are similar to those reported by Lewan (1985) and Lewan and Ruble (2002) for Type II kerogen from the Woodford Shale (see Fig. 2.6). The high HI and low OI measured in the interval sampled for determination of the kinetic parameters are consistent with a Type II or possibly a Type I kerogen (see Table 2.3). The Rock Eval 6, T_{max} reported for these samples suggest that the kerogen is either at, or close to, the level of maturation necessary for intense oil generation (435°C). Furthermore, the production index (PI) which is designed to estimate the amount of petroleum that has been generated by the sample suggests that about 8% of the reactive kerogen has been converted into liquid petroleum.
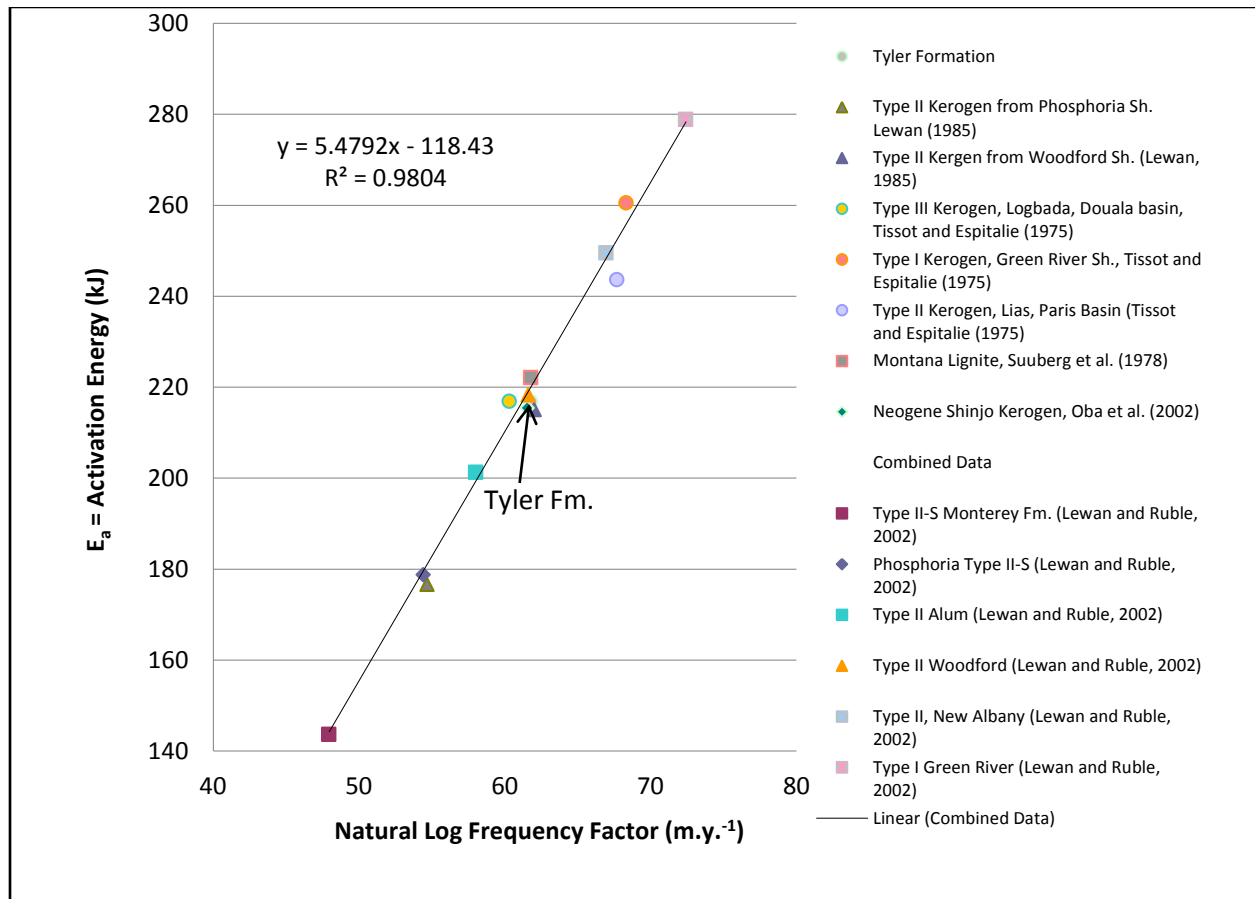
Figure 2.6. A graph illustrating the distribution of published activation energies and natural log of the frequency factor. The kinetic parameters for the Tyler Formation sample from the Harmon 1-26 is highlighted by the arrow.

Table 2.3. Rock Eval 6 results from the interval used to find the kinetic properties of the Tyler Formation in the Harmon 1-26.

NDIC	Depth	LECO TOC	S1	S2	S3	Tmax	HI	OI	PI
10931	7845	32.827	7.89	104.06	2.33	431	316.9951	7.097816	0.070478
10931	7810.7	30.175	11.8	113.17	2.09	435	375.0456	6.926263	0.094423
Drilled with salt-starch mud.									

Kinetics Based Time-Temperature Index

The thermal history developed here uses the preserved stratigraphic section and established ages to reconstruct the burial and temperature history of the Tyler Formation. If the geothermal heat flow and thermal conductivity of the various units involved have been constant then the thermal maturation of the Tyler Formation may be estimated by summing the amount of maturation that has occurred during each of the time-stratigraphic intervals used.

The approach used by Wood (1988), is similar to the Lopatin method with one important difference. The kinetics of kerogen maturation, as defined by Lopatin (1971), does not account for differences in maturation rates caused by variations in kerogen composition. Wood recognized this problem and developed a maturation model that is capable of taking into account kerogen dependent variations in activation energy. This is done by using the Arrhenius equation to describe the chemical reaction rates that are controlled by the composition of the kerogen and the thermal history of the source bed. The standard Arrhenius equation is only valid for isothermal reactions. However, Wood applied a version of the Arrhenius equation developed by Gorbachev (1975) to solve for the reaction progress that occurs when temperatures change at a constant rate. Wood uses the following expression for this purpose:

Eq. 2.7 TTI_{Arr} (t_n to t_{n+1} where $T_n <> T_{n+1}$) = $A/\beta\{[RT^2_{n+1}/(E_a+2RT_{n+1})e^{-Ea/RT_{n+1}}] - [RT^2_n/(E_a+2RT_n)e^{-Ea/RT_n}]\}$

Where:

TTI_{Arr} is a measure of maturation for a kerogen for the time-period t_n to t_{n+1} where the temperature changes from T_n to T_{n+1}.
t = time (m.y.)
T = Temperature (^oK)
A = Frequency factor (m.y.$^{-1}$)
$\beta = \Delta T/\Delta t$ = Heating rate (^oK/m.y.)
R = Gas constant (0.008314 kJ/^oK-mol)
E_a = Activation energy (kJ/mol)

When the temperature history of the source bed is known then estimating the temperature of the source bed before and after each new unit is added (or removed) provides the input needed to solve Eq. 2.7 for the degree of maturation that occurred within the Tyler Formation as each new unit was added. These temperatures and the associated time intervals, when used in Eq. 2.7, provide the incremental change in kerogen maturation that, when summed, yields an estimate of overall maturation (ΣTTI_{Arr}). When petroleum generation involves a first order reaction then the fraction of the original kerogen that remains is related to the ΣTTI_{Arr} (see Wood, 1988) as follows:

Eq. 2.8 $$X = e^{(-\Sigma TTIArr)}$$

      Where:

            X = Fraction of the original kerogen (initially assumed to be 1) that remains.
            ΣTTI_{Arr} = The degree of maturation from Eq. 2.7

Table 2.3 presents the Time-Temperature Index and the fraction of the original kerogen reacted using data from the Rauch Shapiro 21-9 in Eq. 3, Eq. 5 and Eq. 6. The results of these calculations suggest that 7% of the original kerogen has been converted to petroleum.

Formation	Depth (ft.)	Age (m.y)	Thickness (m)	Thermal Conductivity	Δ Temp (°C)	Temperature at base of the Tyler Fm. (°K)	Heating Rate (°C/m.y.)	TTI Arr	1-X - Fraction of Kerogen Converted
Surface	0	0	-61.570	1.720	-2.331	378.4	-0.042	0.074	0.071
Sentinel Butte	-202	55.7	589.788	1.720	22.330	380.7	1.370	0.006	0.006
Pierre	1733	72	989.686	1.720	37.470	358.4	1.338	0.000	0.000
Mowry	4980	100	125.882	1.620	5.060	320.9	0.195	0.000	0.000
Inyan Kara	5393	126	137.465	1.800	4.973	315.8	0.355	0.000	0.000
Swift	5844	140	289.560	2.350	8.024	310.9	0.134	0.000	0.000
Spearfish	6794	200	356.311	2.100	11.049	302.8	0.099	0.000	0.000
Tyler	7963	312	55.778	3.040	1.195	291.8	0.199	0.000	0.000
Big Snowy	8146	318	137.160	2.680	3.333	290.6			

Table 2.4. Example of applying Eq. 2.2, Eq. 2.6 and Eq. 2.7 to determine the level of thermal maturity within the Tyler Formation using data from the Rauch Shapiro 21-9 contained in Table 2.1.
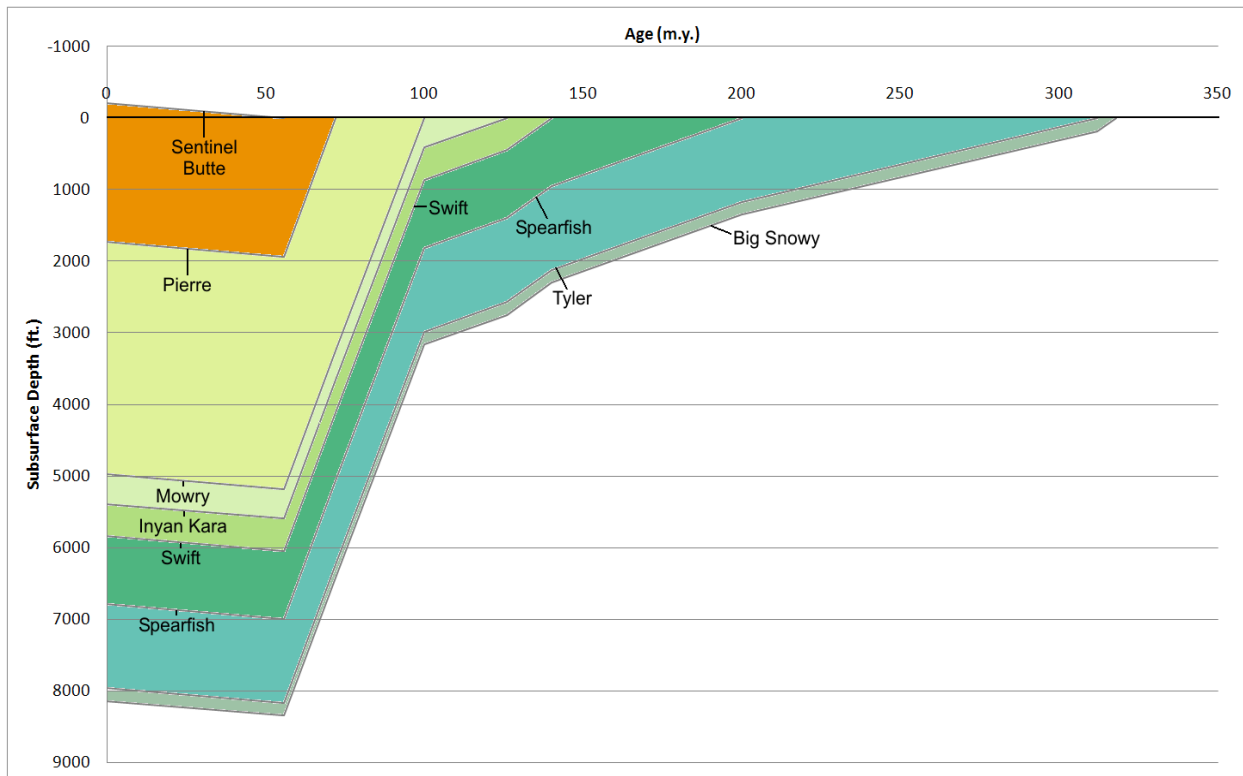

Figure 2.7. Burial history of the Tyler Formation determined from formation tops present in the Rauch Shapiro 21-9 relative to the modern land surface (Subsurface Depth = 0).

27

Basin Model of Tyler Maturation

The procedure used to estimate the level of maturation within the Rauch Shapiro Fee 29-1 can be extended to the basin scale by replacing the single heat flow and unit thicknesses with grids based on maps of these factors. Each of the grids used are registered to each other with depth so that for each grid node there is a heat flow and interval thickness that corresponds to the formations listed in Table 2.1. With this information the calculation of formation temperature, heating rate and an estimate of kerogen conversion rate may be obtained for each grid node as if it were a single well. Summing the conversion rates though time for each grid node leads to an estimate of the total fraction of the reactive kerogen converted. This results in kerogen conversion values that when mapped details the level of maturation that could be expected for the assumed kerogen within the Tyler Formation at the basin scale (see Fig. 2.8).

The procedure used replaces the unit thicknesses in the Rauch Shapiro Fee 29-1, with isopach values. Maps of the isopachs used are contained in the appendix. To simplify the analysis, the values that describe the thermal conductivities and ages of the mapped units in Table 2.1 are assumed to be constant across the basin.

The map generated by this method indicates that there are three areas within the Tyler Formation of North Dakota that may have been matured to the point of generating oil. These areas include a small portion of Divide County that appears to extend into Montana. Two larger areas are also present with one being situated in the deepest portion of the basin in central McKenzie and northwestern Dunn counties and a second located along the southern flank of the basin in Billings, Stark and Hettinger counties. It should be noted that these more mature areas correspond well with areas of high heat flow (Fig. 2.1). This suggests that variations in heat flow are more important with regard to maturation than is depth.

In order to evaluate the maturation levels presented in Fig. 2.8, samples of cuttings and core were collected and analyzed by the Rock-Eval method. The average T_{max} value is posted next to the well head of the sampled well. The value of T_{max} is particularly relevant to studies of source rock maturity. In general, intense oil generation is considered to begin when Rock-Eval T_{max} values are greater than $435^{o}C$ and ends when Rock-Eval T_{max} exceeds $470^{o}C$ (Peters and Cassa, 1994) . However, the precise onset and end of oil generation may vary from these values depending upon the composition of the kerogen involved. T_{max} is the temperature that corresponds with the most intense generation of hydrocarbons during programmed pyrolysis. However, for reasons based on the placement of the temperature measuring thermocouples in the original Rock-Eval machines, the Rock-Eval T_{max} is about $40^{o}C$ less than the temperature that actually generates the peak in hydrocarbon formation. However, the temperature correction is designed to make data consistent even though the data was obtained using different machines.

In order to reconcile these differences, additional work and data will be needed. Given that the theoretical degree of maturation is closely related to the geothermal heat flow, one likely source of error would be in the current heat flow map. A second source of error would be in the lack of

stratigraphic data for the post-Sentinel Butte section. This interval is particularly important because the most critical oil generation phase within the Tyler Formation appears to have begun after deposition of the Sentinel Butte. Another source of error could be expected to involve the naïve assumption that all of the kerogen within the Tyler Formation is essentially the same. This assumption is clearly challenged by the significant variation in depositional environments that produced the three broad facies tracts outline earlier. Consequently one could expect significant variation in kerogen type and reactivity based on the prevalent set depositional facies. However, in spite of these weaknesses, there is considerable agreement between regions that show a theoretical expectation of oil generation and T_{max} values that indicate the same. There are two areas in particular that exhibit this coincidence. The first is situated in McKenzie and Dunn counties and the second is in centered in Billings, Slope and Hettinger counties. Oil production from both of these areas, especially the second, lends additional credibility to the oil generating potential of the Tyler Formation.
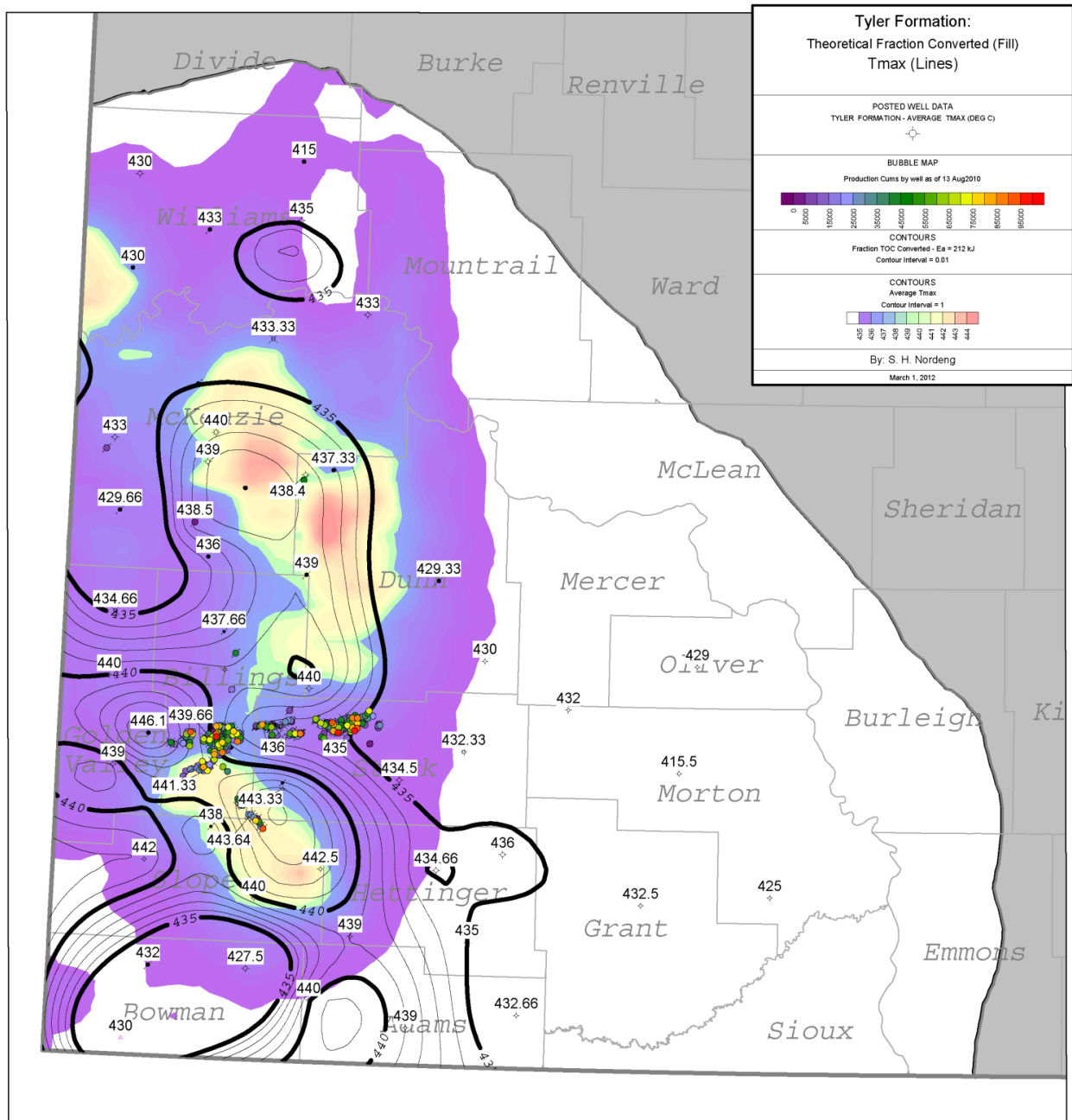
Figure 2.8. Map of the western half of North Dakota showing the fraction of reactive kerogen within the Tyler Formation that has been converted to petroleum. The posted values are the average T_{max} values obtained from Rock-Eval pyrolysis. Wells that have produced from the Tyler Formation are shown as the color filled circles with the colors keyed to the initial production of these wells. Most of the wells lie along the east-west Dickinson-Fryburg trend.

Shale Resistivity

Electrical resistivity studies of the Bakken shale (Meissner, 1978) show a relationship between elevated resistivity and source rock maturation. This effect is believed to result from the expulsion and replacement of interstitial water by generated oil within the source shale. Natural formation water typically has high concentrations of dissolved salts which conduct an electrical current. Oil, however, is a poor conductor. These properties of oil and formation water cause water-saturated shale to be electrically conductive (low resistivity) and oil-saturated shale to be electrically resistive (high resistivity). Meissner (1978) suggested that when the resistivity of the Bakken Shale is greater than 30 Ω–m the shale is oil-saturated and therefore thermally mature.

This study applies the shale resistivity model to the Tyler Formation. In the northern parts of the basin, maximum resistivity values were taken from one of the high gamma ray intervals (>150 API) within the Tyler (Fig. 2.9). These intervals were selected because the high gamma ray intervals correlate with organic-rich shale in core and they appear to show an increase in resistivity at depth. In the southern study area, south of the Dickinson-Fryburg Trend, the high gamma ray intervals are absent. The maximum shale resistivity was recorded from the Tyler Formation for over three hundred wells (Fig. 2.10) and contoured using the logarithm of the most resistive shale found in the Tyler Formation.

Southern Williams, northwestern Dunn, and most of McKenzie counties (Fig. 2.10) contain the highest shale resistivities. This area corresponds with where the Tyler Formation is at its greatest depths in the Williston Basin and contains the high gamma ray shale intervals (well #6846, Fig. 2.9), interpreted to be off-shore, organic-rich marine shale. Based on the resistivity data, the organic rich source beds in the Tyler Formation could be oil-saturated throughout west-central North Dakota.

Some of the high to low resistivity transitions within Figure 2.10 are a function of lithology change while others are related to depth.   Three high gamma ray intervals extend across most of McKenzie County and the surrounding area, but do not extend into southwestern North Dakota (e.g. well #4849, Fig. 2.9). The maximum resistivity along the high gamma ray intervals (e.g. well #6846, Fig. 2.9) increases from ~10-20 Ω–m in Williams County to greater than 1,000 Ω–m in central McKenzie County (Fig. 2.10). The increase in resistivity correlates with thermally maturing organic-rich shale within the Tyler Formation. Therefore the southward increase in maximum shale resistivity in west-central North Dakota for the Tyler Formation is probably a function of thermal maturity.

Moving away from the McKenzie County area, the high gamma ray shale intervals pinch out and the Tyler Formation typically only contains shale with a moderate gamma ray signature (~100-125 API). The decrease in gamma ray signature could coincide with lower TOC content and/or a difference in source rocks within the Tyler between west-central and southwestern North Dakota. Another possibility is that the source rocks in the southwest are surrounded by permeable rock layers that have allowed enough migration of generated hydrocarbons so that there is formation water still in place to conduct significant electricity.
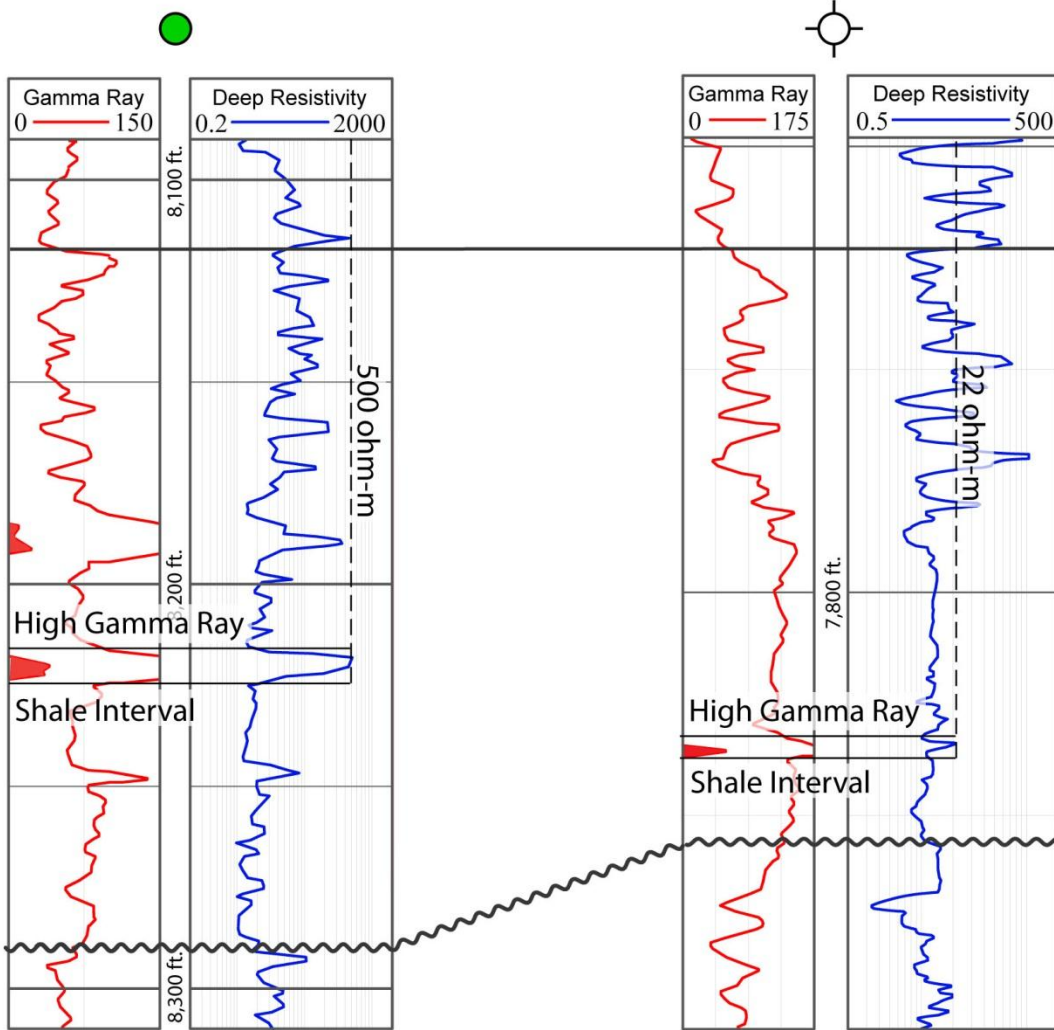
Figure 2.9. Stratigraphic cross-section of the Tyler Formation displaying how the maximum shale resistivity was determined on a well by well basis. The locations of the above wells are shown on Figure 2.10.
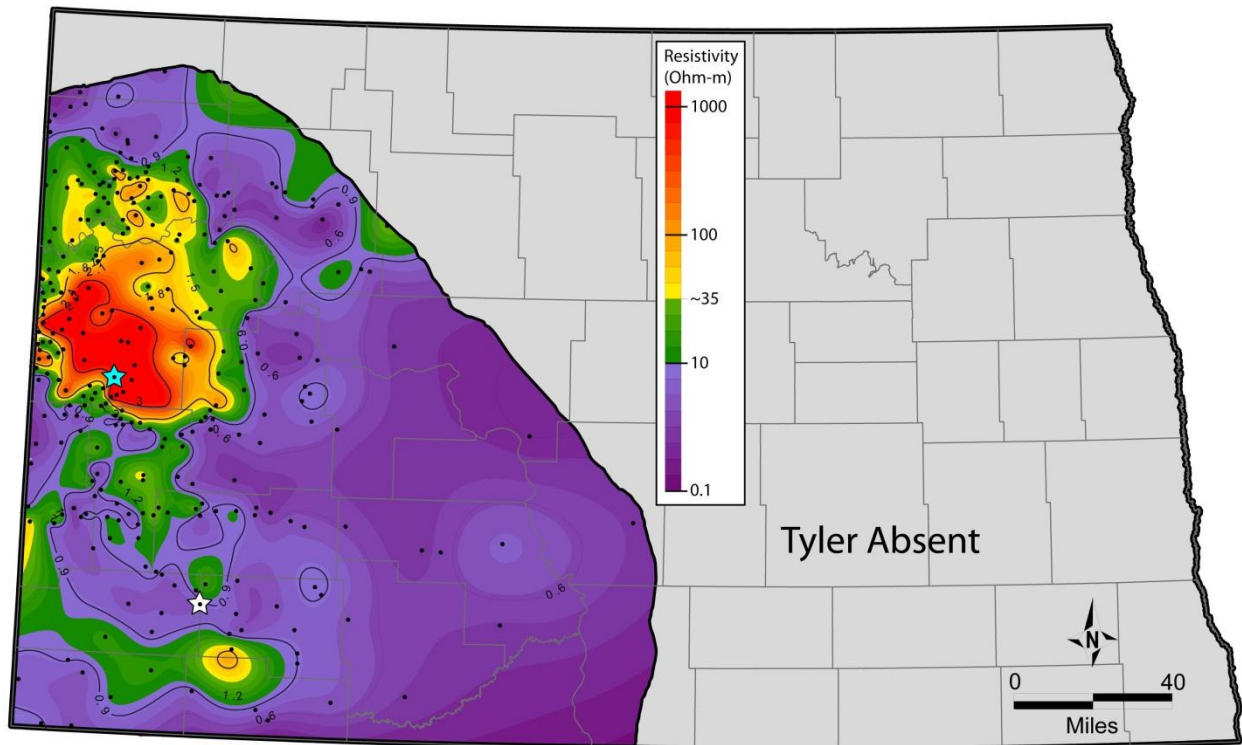
Figure 2.10. Shale Resistivity Map of the Tyler Formation. The blue star shows the location of well #6846 in Figure 2.9 and the white star shows the location of well #4849.

3) Oil Expulsion & Accumulation

The Tyler Formation contains organic-rich, oil-prone source beds that are thermally mature. The distribution of organic matter within the Tyler section varies throughout the state. In the west-central part of the state, the lower portion of the Tyler contains up to three organic-rich black shale intervals (Fig. 3.1). Towards the south, the organic-rich shale intervals in the lower Tyler pinch out while an interval of interbedded organic-rich shale and limestone appears in the upper Tyler (Fig. 3.1). The question, however, is whether the expelled oil has accumulated within the Tyler system, trapped by low permeable seals, or if it has migrated out of the system.

Fluid pressure analysis is one method that can be used to gain insight into source rock maturation and hydrocarbon migration. Most sedimentary rock intervals within the Williston Basin have hydrostatic (normal) fluid pressure gradients, which are 0.43 psi/ft. for fresh water and 0.46 psi/ft. for salt water. A hydrostatic pressure gradient is caused by the weight of the overlying water column. Hydrostatic pressure indicates that a formations fluid system is in "open" hydraulic communication with surrounding strata all the way to the surface and has reached pressure equilibrium. An abnormal fluid pressure gradient (≠ 0.43-0.46 psi/ft.) indicates a formation has a "closed" fluid system. A "closed" fluid system occurs when low to impermeable layers either seal off a formations fluid system from hydraulic communication with the surrounding strata or temporarily impede pressure equilibration. Intense oil generation in a "closed" fluid system is one process that can cause abnormally high fluid pressures and is summarized in Figure 3.2.

Regarding hydrocarbon generation and fluid overpressure, there are two schools of thought: the static school and the dynamic school (Bredehoeft et al., 1994). The static school believes that fluid overpressure can be caused by hydrocarbon generation and maintained indefinitely by impermeable seals (Hunt, 1990; 1991). The dynamic school, however, does not believe in impermeable rocks, noting that all rocks are permeable to one degree or another (Toth et al., 1991; Bredehoeft et al., 1994). Therefore, according to the dynamic school, fluid overpressure is only maintained for extended periods of geological time when hydrocarbon generation is continuous (Toth et al., 1991) and once hydrocarbon generation has ceased, fluid pressure will eventually re-equilibrate to a hydrostatic pressure. While there may not be a consensus regarding the sustainment of fluid overpressure, there is agreement that fluid overpressure can be caused by intense hydrocarbon (oil) generation.

The Bakken Formation of the Williston Basin is one example of a formation that contains thermally mature source rocks bounded by impermeable seals resulting in fluid overpressure. Meissner (1978) examined fluid pressures within the Bakken Formation and found that in the shallower areas of the Williston Basin, where the Bakken does not produce significant oil and gas, the fluid pressure gradient is ≈ 0.46 psi/ft. In the deeper parts of the Williston Basin, where the Bakken Formation now produces economically extractable oil and gas, Meissner found fluid pressure gradients in excess of 0.76 psi/ft. He explained this by suggesting that over-pressurization is the expected result when intense oil generation occurs between poorly permeable beds that form a closed hydraulic system. Therefore the presence of overpressurized conditions may be a key element in defining the existence and extent of a regional scale resource play.
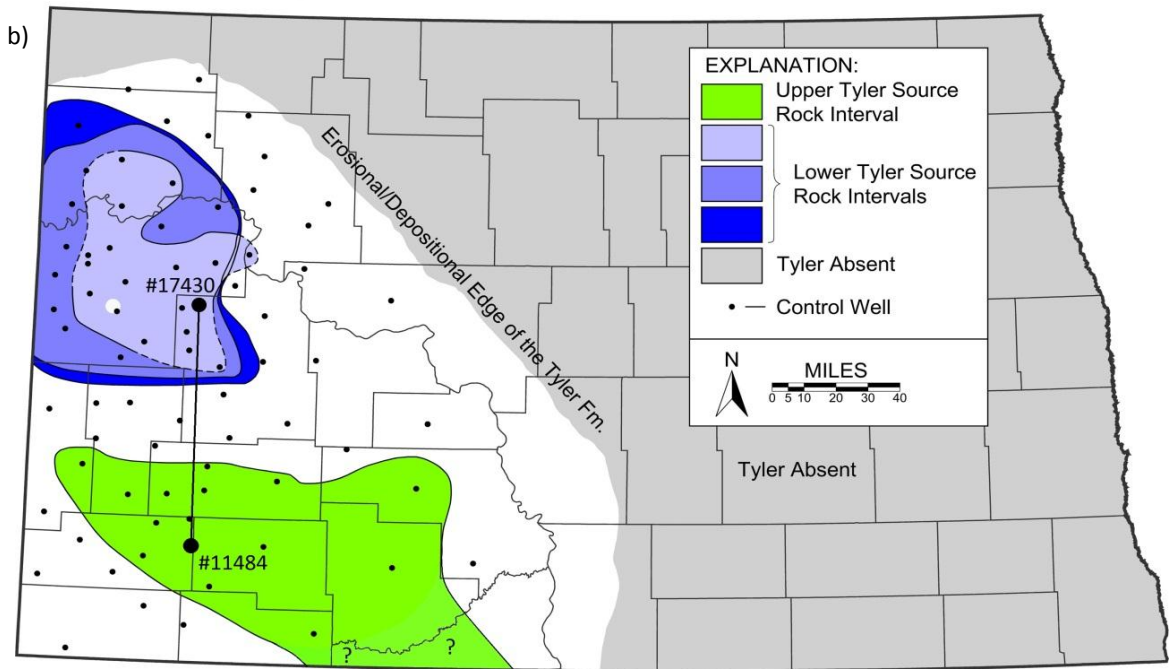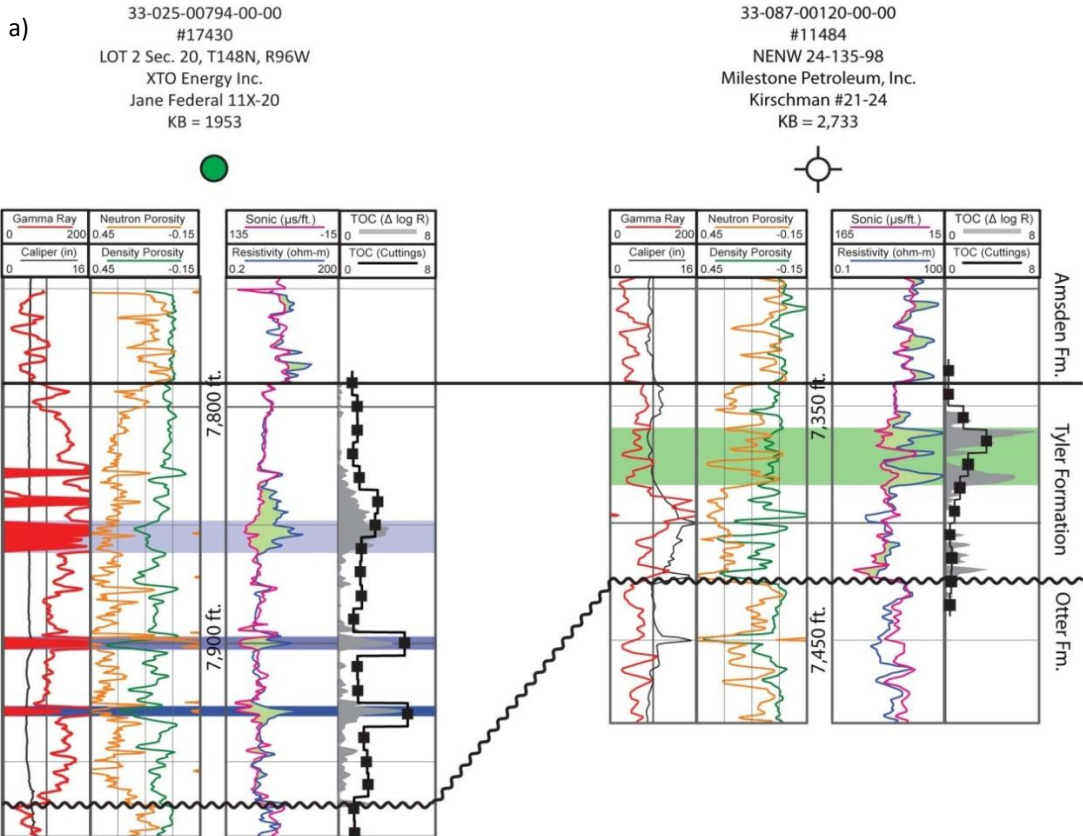
Figure 3.1. Tyler source rock information. a) Cross-section depicting interpreted potential source rock intervals. "TOC (Cuttings)" represent TOC weight percentage measured off or drill cuttings. "TOC (Δ Log R)" was calculated using the Passey method (Passey et al., 1990).   B) Map showing the approximate extent of source rock intervals from the above cross-section. Mapping was completed using TOC wt. % measured from drill cuttings and/or calculated using the Passey method.

Model for Intense Oil Generation Induced Fluid Overpressure

Immature

(Initial Source Rock Thickness)

Organic-poor rock with low permeability and porosity

Organic-rich shale with low permeability and porosity

Organic-poor rock with low permeability and porosity

Prior to maturation, both the source rock (organic-rich shale) and surrounding rock is saturated with formation water. The formation water is in equilibrated hydraulic communication with the surface and the fluid pressure is normal (hydrostatic).

Early Mature

Source rock compresses

Generated oil begins to displace water

Oil generation begins: Kerogen (solid) converts to oil (fluid) decreasing the amount of solid material in the rock which results in compaction. The generated oil increases the fluid density and displaces the natural formation water from the source rock (organic-rich shale). The fluid pressure begins to increase due to compaction and an increase in fluid density.

Mature

Compression continues

Displacement continues

During continued maturation (oil generation), the rock surrounding the source rock becomes charged with oil. The low permeability and porosity of the surrounding rock minimizes oil migration which leads to an increase in fluid pressure within the entire immediate system.

Explanation

- Non-organic (detrital)

- Carbonate grain

- Kerogen (organics)

- Oil

- Water

Figure 3.2. Schematic diagram depicting fluid displacement and source rock compaction during hydrocarbon generation, modified after Meissner (1978).

Methods

Tyler Formation fluid pressures were examined to differentiate areas with normal, hydrostatic fluid pressure gradients (~0.46 psi/ft.) from areas with abnormally high fluid pressure gradients (>0.46 psi/ft.). This study examined pressure data from 30 drill stem tests run on the Tyler Formation in western North Dakota (Table 3.1). A drill stem test (DST) is a procedure used to determine the productive capacity, pressure, permeability, and/or extent of a hydrocarbon. The DST's examined in this study were run on either wildcat wells, wells in established fields that did not substantially produce from or inject into the Tyler, or wells within producing Tyler fields that were drilled and tested prior to or shortly after field production began. In order to examine the original virgin fluid pressure of the Tyler Formation only DST's that may had not been compromised by fluid production and/or injection were used. Approximate Tyler Formation fluid pressures were calculated using the Horner plot method (Horner, 1951), which extrapolates a formation's fluid pressure using DST time-pressure data (e.g. Fig. 3.3). Fluid pressure gradients (psi/ft.) were calculated by dividing the extrapolated fluid pressure (psi) by the depth to the top of the DST interval (ft.).
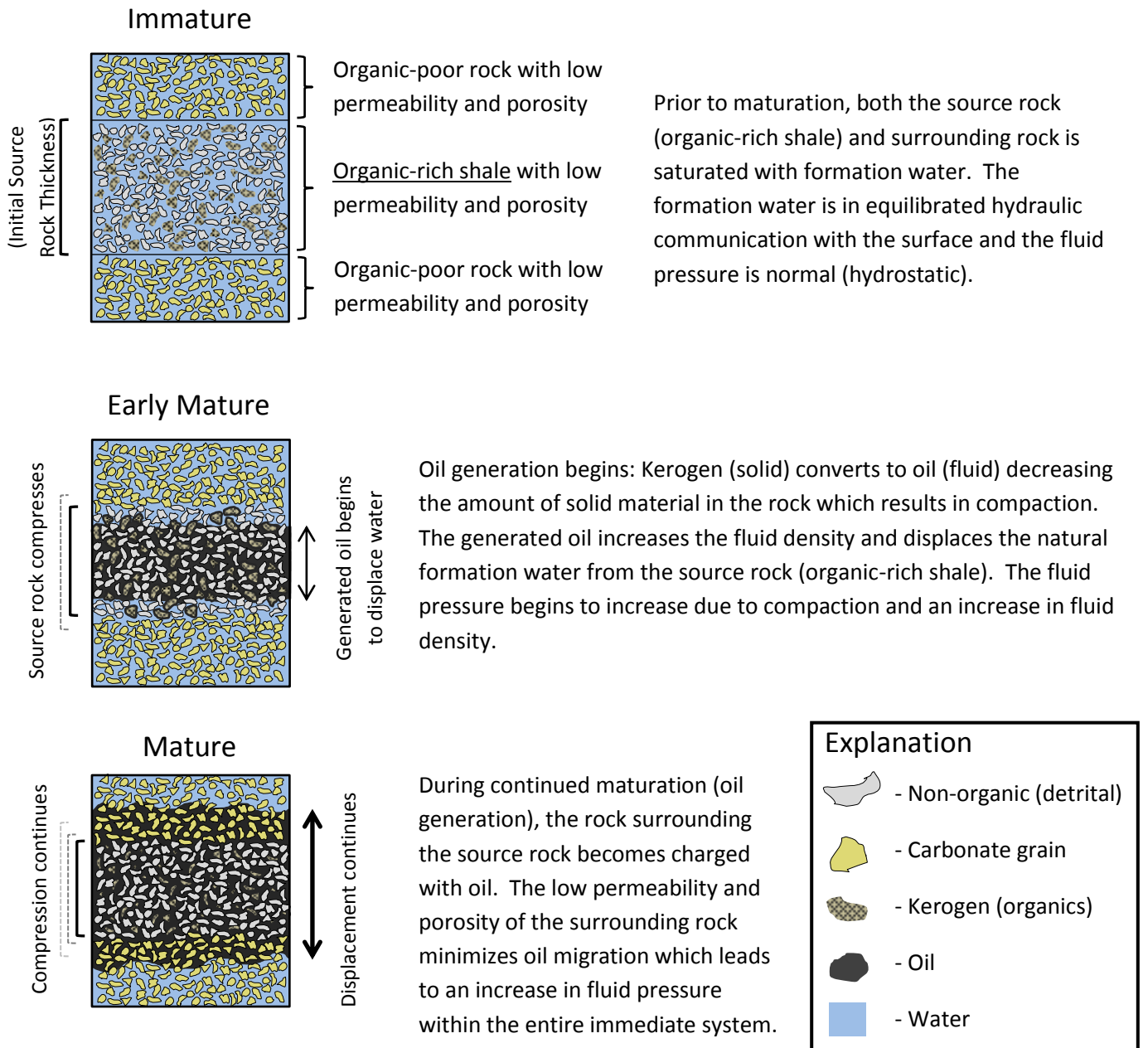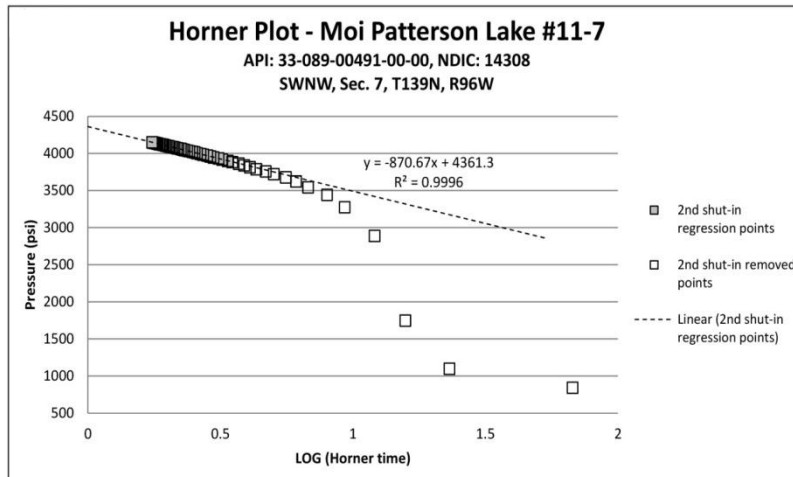

Figure 3.3. Horner plot example showing time-pressure data measured during the 2nd shut-in period of an open hole drill stem test (DST) on the Tyler Formation (7,762-7,785 ft. M.D.) from Burlington Resources Moi Patterson Lake #11-7. The extrapolated fluid pressure (Horner, 1951) from the DST is ~4,361 psi at a depth of 7,762 ft., which yields a pressure gradient of 0.56 psi/ft.. The fluid pressure extrapolated from the 1st shut-in period was 4,259 psi (0.548 psi/ft.). The fluid recovered in this test was 1,020' of gas cut mud and 627' of highly oil and gas cut mud. Moi Patterson Lake #11-7 has produced over 130,000 barrels of oil, 2,700 MCF of gas, and 1,000 barrels of water.

Equation 3.1

$$\text{LOG (Horner Time)} = \text{LOG} \left[\frac{(T + \Delta t)}{\Delta t} \right]$$

Where:

    T = cumulative elapsed time during the open flow period/s prior to the shut-in period
    Δt = amount of elapsed time during the shut-in period

Results

Ten of the DST's examined showed the Tyler Formation to have abnormally high fluid pressures (> 0.46 psi/ft.) while the other twenty showed Tyler Formation fluids to be at hydrostatic pressure (~0.43-0.46 psi/ft., Table 3.1). Of the ten DST's that exhibit overpressure, six of them cluster together in southwestern North Dakota and the other four define a northern area of overpressure in west-central North Dakota (Fig. 3.4). The extrapolated fluid

NDIC Well #	API	BHT (°F)	Test Interval Top	Test Interval Bottom	Interval Length (ft)	Fluid Pressure (psi)	Pressure Gradient (psi/ft)	Tyler Fm. Top TVD	Tyler Fm. Top SSLD	DST Fluid Recovery Water	DST Fluid Recovery Mud	DST Fluid Recovery Oil
919	3305300069		7430	7483	53	*3275	*0.439	7271	4901	1470		
1926	3304100002	158	6835	6866	31	3048	0.445	6814	4265	5580		
3339	3300700056	221	8026	8057	31	4317	0.537	7996	5390	500	60	
4575	3308900067	216	8079	8125	46	3582	0.442	8036	5461	6350	**470	
4851	3308900095	234	7974	7996	22	*4158	*0.523	7906	5123		**31	7904
4920	3308900105		8215	8300	85	3626	0.437	8206	5579	3704		
5104	3303300035	216	7766	7820	54	3451	0.443	7730	5278	5828		
5157	3302500044		7838	7926	88	*3698	*0.469	7762	5551	6951	226	
5167	3303300036	208	7833	7868	35	3599	0.458	7754	5311		225	
5243	3300700152	214	7985	8136	151	4007	0.497	7963	5322	3090		
5274	3302500048	168	7504	7553	49	3462	0.460	7464	5209	2632	172	
5282	3308900135	192	7743	7750	7	3471	0.448	7651	5149	6292		
5399	3302500052	196	8101	8231	130	3701	0.456	7977	5372	7180		
5477	3308900164	170	7637	7674	37	3452	0.453	7572	5105	6664	186	
5567	3301100194		6180	6246	106	2769	0.447	6252	3247	354	91	
5722	3303300040	222	7844	7871	27	3371	0.429	7783	5003	6901		
5754	3308900196	178	7447	7586	139	3351	0.449	7421	4971	1741		
6846	3305300859	222	8180	8282	102	4541	0.552	8174	5731		**568	
6976	3300700346	210	7607	7669	62	*4054	*0.531	7600	5286		**578	60
7432	3300700472	218	8100	8134	34	3533	0.436	8069	5511	470	277	
8695	3300700722	215	8178	8212	34	4694	0.572	8164	5650		90	360
9815	3302500354	198	8166	8205	39	3693	0.451	8117	5518	14857	653	
10522	3304100032	179	7135	7364	229	3191	0.448	7152	4532	4000	2052	
11298	3308900349	182	7804	7825	21	3438	0.440	7734	5187		144	302
11315	3305301997	214	8431	8563	132	4412	0.519	8475	5819	269	133	2586
11484	3308700120	194	7540	7556	16	3975	0.527	7440	4707	79		5
11510	3303300165	194	7746	7772	26	3470	0.447	7693	5250	72	89	
11525	3303300166	206	7892	7939	47	3460	0.440	7861	5260	4530	643	
14308	3308900491	208	7762	7785	23	4310	0.554	7705	5242		**1647	
15443	3302500566	222	8030	8095	65	*4713	*0.585	7978	5806		**410	56

*Minimum Fluid Pressure/Pressure Gradient   Converted barrels to feet assuming 1 BBLS = 164 ft.

**Oil and/or gas cut mud

Table 3.1. Well and Drill Stem Test (DST) information compiled by this study. Grey shaded rows indicate wells with fluid overpressure in the Tyler Formation and white rows wells with normal fluid pressure.

pressures were compared to sub sea level depth (Fig. 3.5, 3.7b), bottom hole temperature (Fig. 3.6), source rock distribution (3.7a), DST fluid recovery (3.7c), and oil production (Fig. 3.7d) to better understand both the cause and regional extent of fluid overpressure within the Tyler fluid system.
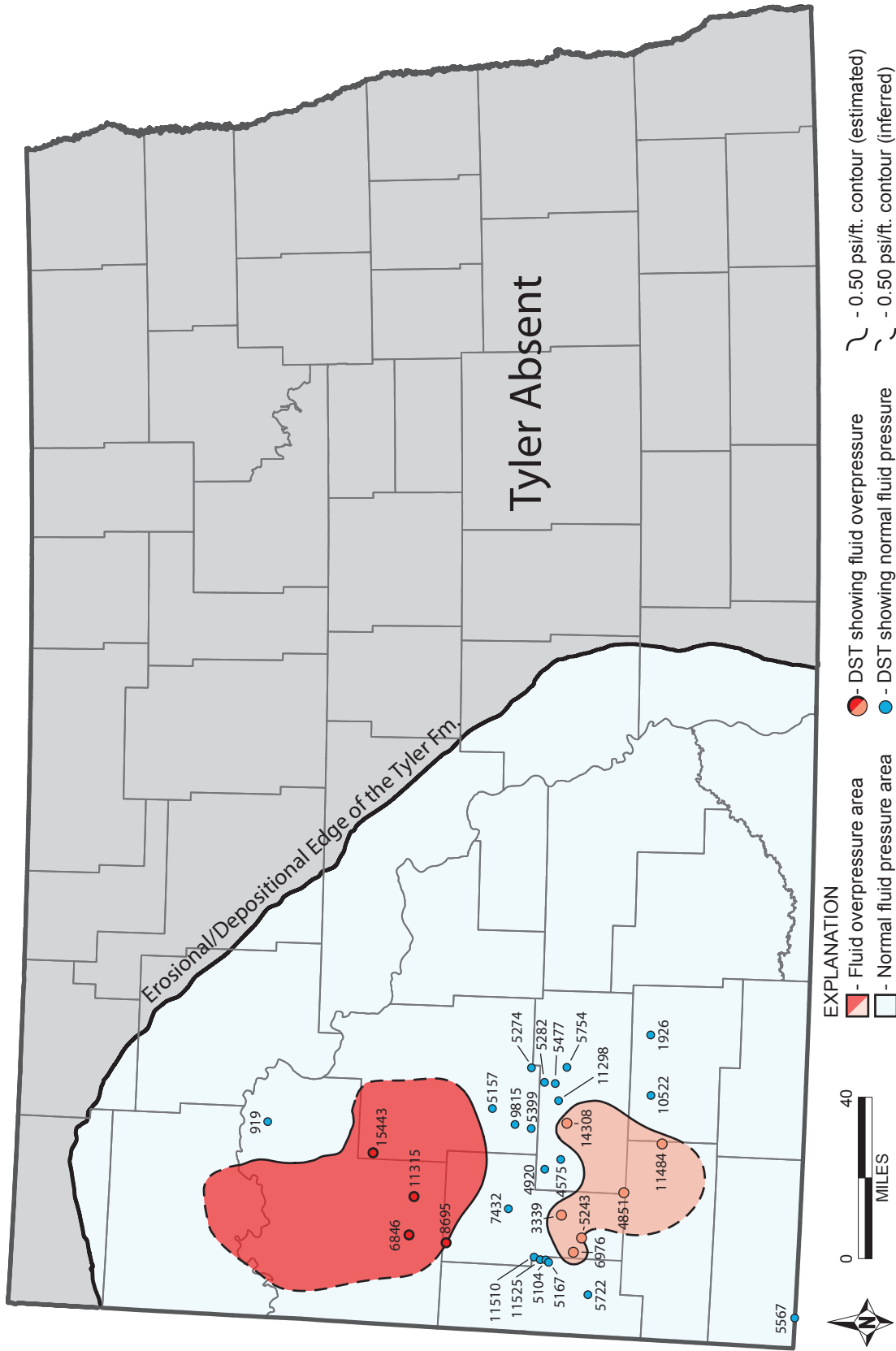
Figure 3.4. Map showing the approximate areas where the Tyler Formation has abnormally high fluid pressure. The fluid pressures used to generated this map were extrapolated from the time-pressure data of 30 drill stem test's (DST's) run on the Tyler Formation from 30 different wells. The wells were either wildcat wells, wells from non-Tyler producing fields, or wells from productive Tyler fields with the DST's run prior to significant production and prior to any injection.
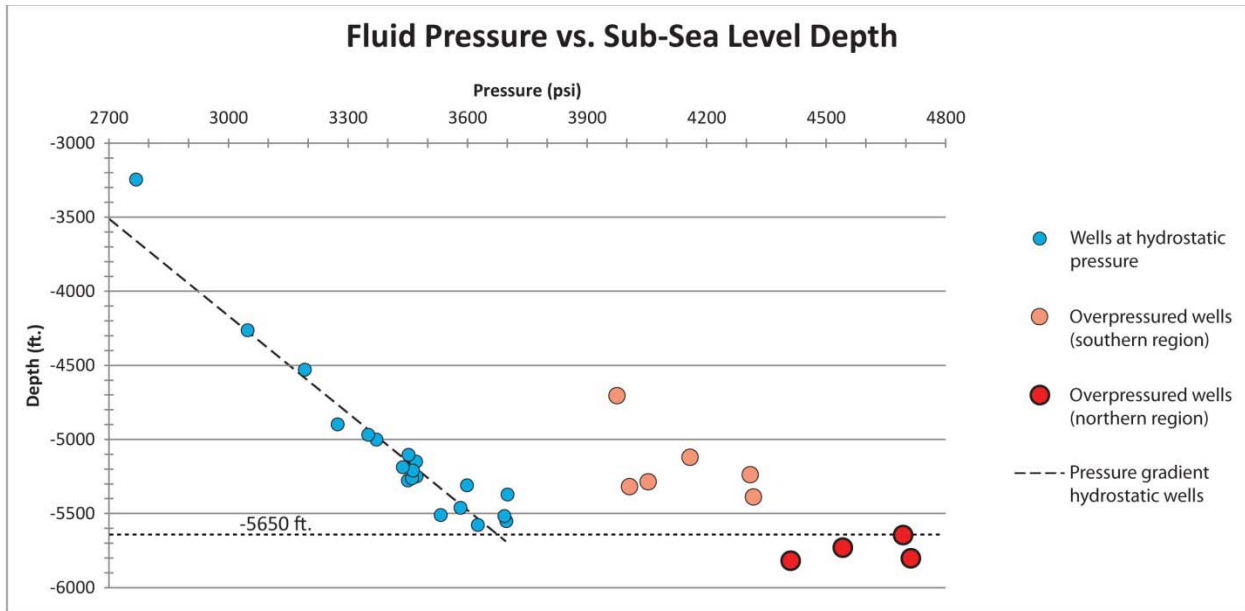
Figure 3.5. Diagram of extrapolated Tyler Formation fluid pressures plotted against the Tyler Formation top sub-sea level depth.
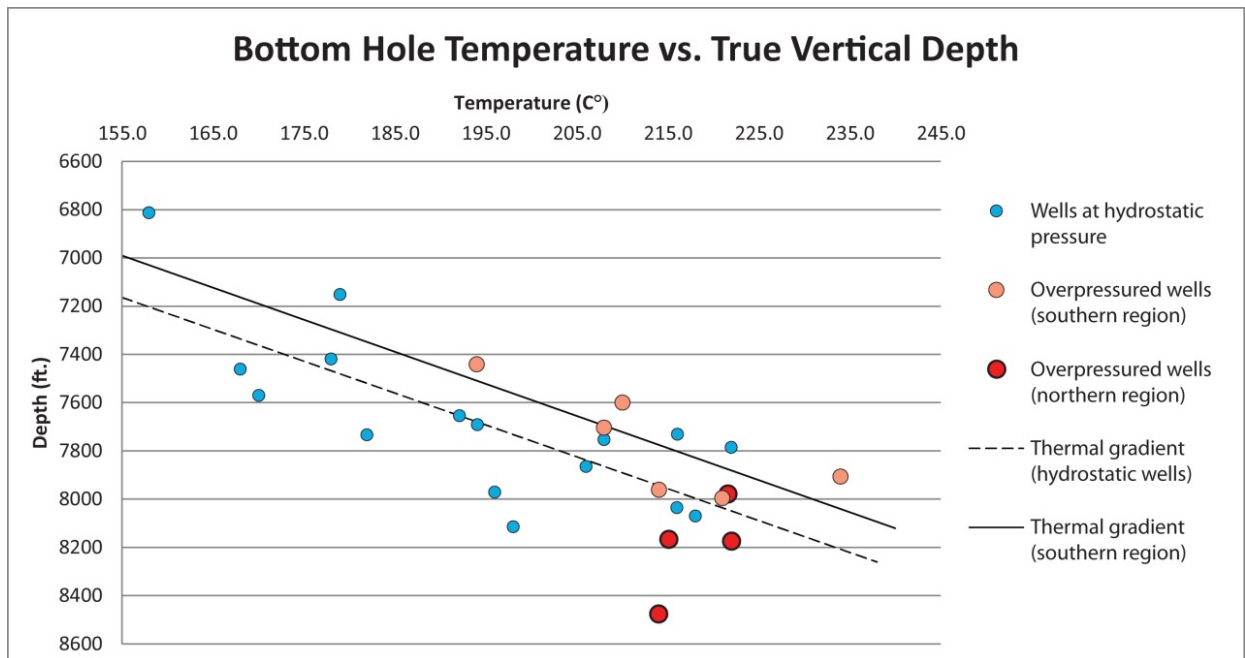
Figure 3.6. Diagram of bottom hole temperatures (measured during the DST) of the Tyler Formation versus depth. The six wells from the southern area of fluid overpressure (light red circles) have a higher thermal gradient (°C/ft.) than the hydrostatic wells (blue circles) and the wells from the northern region of fluid overpressure.
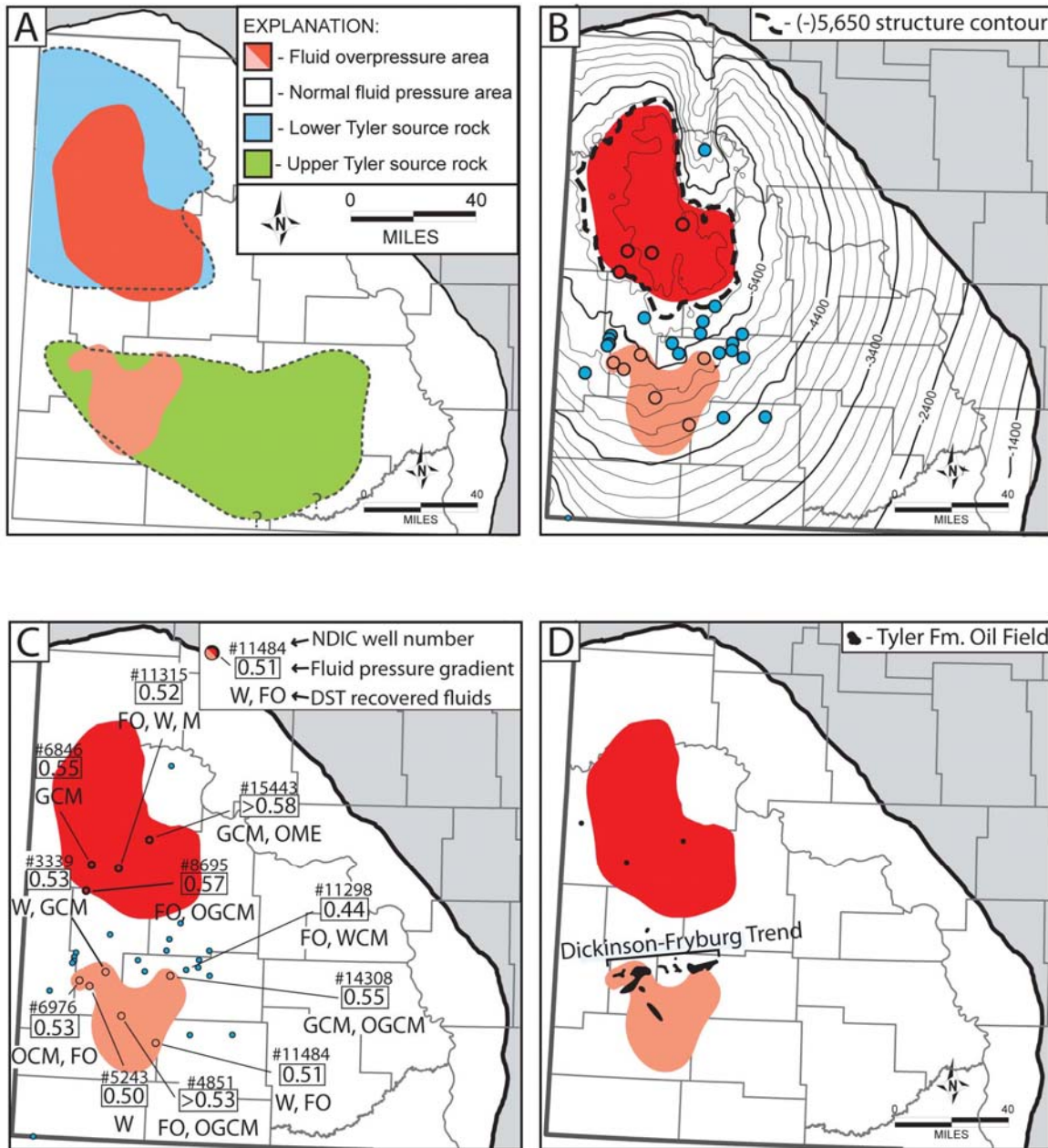
Figure 3.7. Various maps examining the regions of fluid overpressure in the Tyler Formation. a) Comparison of source rock distribution and source rock intervals. b) Structure contour map of the Tyler Formation surface with the approximate areas of fluid overpressure. The northern area of overpressure is defined approximately by the 5,650 ft. (dashed line) contour while the southern area of overpressure is approximated by well control and not depth. c) Fluid pressure map of the Tyler Formation with DST pressure gradients and fluid recovery for the ten wells with fluid overpressure. FO = Free Oil, GCM = Gas Cut Mud, M = Mud, OCM = Oil Cut Mud, OGCM = Oil and Gas Cut Mud, OME = Oil and Mud Emulsion, W = Water, WCM = Water Cut Mud. d) Fluid pressure map with areas of oil and gas production from the Tyler Formation. The Dickinson-Fryburg trend refers to the east-west distribution of productive Tyler oil fields in southwestern North Dakota.

The extent of the northern area of fluid overpressure is poorly defined by DST/well control (Fig. 3.4). However, all four DST's with a Tyler Formation top greater than 5,650 ft. below sea level have a pressure gradient above 0.46 psi/ft. (Table 3.1; Fig. 3.5 and 3.7b), while all off the DST's at hydrostatic pressure have a Tyler Formation top less than 5,650 ft. This depth versus fluid overpressure relation indicates that fluid overpressure in the northern area may be in part a function of sub-sea level depth. Therefore, the extent of the northern area of overpressure is estimated by tracing the ~5,650 ft. sub-sea level depth contour of the Tyler Formation top (Fig. 3.7b).

The southern area of fluid overpressure does not appear to be strictly a function of depth. All six DST's that define the southern area of fluid overpressure have a similar Tyler Formation top depth range as the adjacent DST's at hydrostatic pressure (Fig. 3.5 and 3.7b). The southern area of fluid overpressure was approximated using well control. The average temperature gradient of the Tyler Formation for these six DST's at overpressure, however, is higher than the average temperature gradient of all the other wells (Fig. 3.6). This temperature data suggests that the thermal gradient of the Tyler Formation in the southern fluid overpressure area may be higher than the surrounding areas. The higher thermal gradient may have thermally matured the Tyler Formation in only part of southwestern North Dakota (Fig. 3.4).

Cause of Fluid Overpressure

To test whether fluid overpressure in the Tyler Formation is the result of intense hydrocarbon generation, the DST fluid recovery records were compiled and examined. If fluid overpressure is caused by intense oil and/or gas generation, than the DST fluids recovered from wells with overpressure should contain more oil and/or gas than wells at hydrostatic pressure. Out of the ten DST's that showed fluid overpressure, nine recovered some type of hydrocarbon show such as free oil, gas cut mud, oil cut mud, and/or oil and gas cut mud with minimal water (Table 3.1, Fig. 3.7c). Of the twenty DST's that showed Tyler Formation fluids to be at hydrostatic pressure, only one reported free oil recovery and another very slightly water and gas cut mud (Table 3.1, Fig. 3.7c). In approximately 90% of the tests, Tyler fluids at overpressure contain oil and/or gas while Tyler fluids at normal (hydrostatic pressure) do not. This hydrocarbon-overpressure relationship suggests that fluid overpressure in the Tyler Formation is the result of hydrocarbon generation.

Oil and gas production also correlates with the areas of fluid overpressure. Figure 3.7d displays the areas of Tyler Formation oil and gas production along with the areas of fluid overpressure. The Dickinson-Fryburg trend, where oil and gas is produced primarily from bar-type sand deposits, partially overlaps with the southern area of overpressure (Fig. 3.7d). Two wells have produced oil out of the spatially estimated northern area of overpressure, with a third small producer just to the west (Fig. 3.7d). The overlap between areas of fluid overpressure with oil and gas production further supports the idea that fluid overpressure in the Tyler Formation is the result of intense hydrocarbon generation.

Discussion

There are three components necessary to produce oil generation induced fluid overpressure within the Tyler Formation: 1) sufficient quantities of kerogen to source oil and/or gas, 2) thermal maturation of kerogen to generate oil and/or gas, and 3) hydraulic seals both above and below the organic-rich intervals to minimize hydrocarbon migration. Without thermally matured kerogen, there would be no source for the additional fluid and/or gas necessary to cause overpressure. Also, without sufficient seals, substantial amounts of generated hydrocarbons would be able to migrate from the system and the fluid pressure would return to the hydrostatic gradient. Therefore, fluid overpressures observed indicate the Tyler Formation contains thermally mature source rocks that are bounded above and below by low to impermeable rocks.

Areas, or zones, of fluid overpressure are not only defined by lateral, horizontal boundaries, but also by vertical boundaries. Figure 3.8 displays a series of logs from Pennzoil Company's Grassy Butte #21-23F (NDIC: 11315) along with vertically interpreted pressure domains based on oil shows in the drill cuttings. The DST interval from well #11315 extended across both the interpreted zones of fluid overpressure and normal pressure (Fig. 3.8). The fluid pressures recorded during the DST could be pressure values intermediate between the normal and overpressure zones.

The extrapolated fluid pressure gradients within the two regions of overpressure vary in part due to variation in DST length and stratigraphic location. Figure 3.9 displays two cross-sections, one in the northern region of fluid overpressure (Fig. 3.9a, A-A') and the other in the southern region (Fig. 3.9b, B-B'). In cross-section A-A' (Fig. 3.9a), all three DST's extend across portions of the Tyler Formation and show fluid overpressure (Fig. 3.9a). However, the DST from #11315 extends above the proposed zone of overpressure by 30-50 ft. while the DST from well #6846 may extend 10-30 ft. below the overpressure zone (Fig. 3.9a). The DST's from wells #6846 and #11315 may have produced intermediate fluid pressure readings, between the overpressure and normal pressure zones. Each of these two wells has a pressure gradient significantly below that of well #15443, which had its DST run entirely in the proposed zone of overpressure (Fig. 3.9a). Therefore, the fluid pressure gradient of these three wells in the northern region of fluid overpressure may vary in part because of differences in location and interval length between the DST's.

In the southern region of fluid overpressure, fluid overpressure probably centers around the organic-rich upper portion of the Tyler section. In the southwest, Tyler DST's commonly target the upper portion of the section (e.g. well #6976 in Fig. 3.9b), where productive sand interval/s are most often found. TOC (Total Organic Carbon) measurements off of drill cuttings (e.g. well #11484, Fig. 3.9b) indicate the upper Tyler is rich in organic material, and is therefore capable of generating oil and/or gas, while the lower Tyler is more organic-lean. High oil saturations from core analysis (e.g. well #4849, Fig. 3.9b) suggest the upper Tyler source rocks have generated oil that is still in place within upper Tyler limestone beds.

Figure 3.8. Compilation of several vertical logs of the Tyler Formation from Pennzoil Company's Grassy Butte #21-23F (NDIC: 11315, API: 33-053-01997-00-00), including (moving left to right): gamma ray and resistivity logs, a lithological log along with a record of several types of oil shows borrowed from the well file geologic report, a vertical schematic fluid pressure profile, and the DST Interval. The zone of fluid overpressure was modeled to extend along the vertical extent of oil shows within the drill cuttings, and normal fluid pressure wherever there were no shows. The transition from overpressure to normal pressure is speculated to be gradational, with a transitional pressure zone between the normal and overpressure zones, but it may be non-gradational and abrupt.
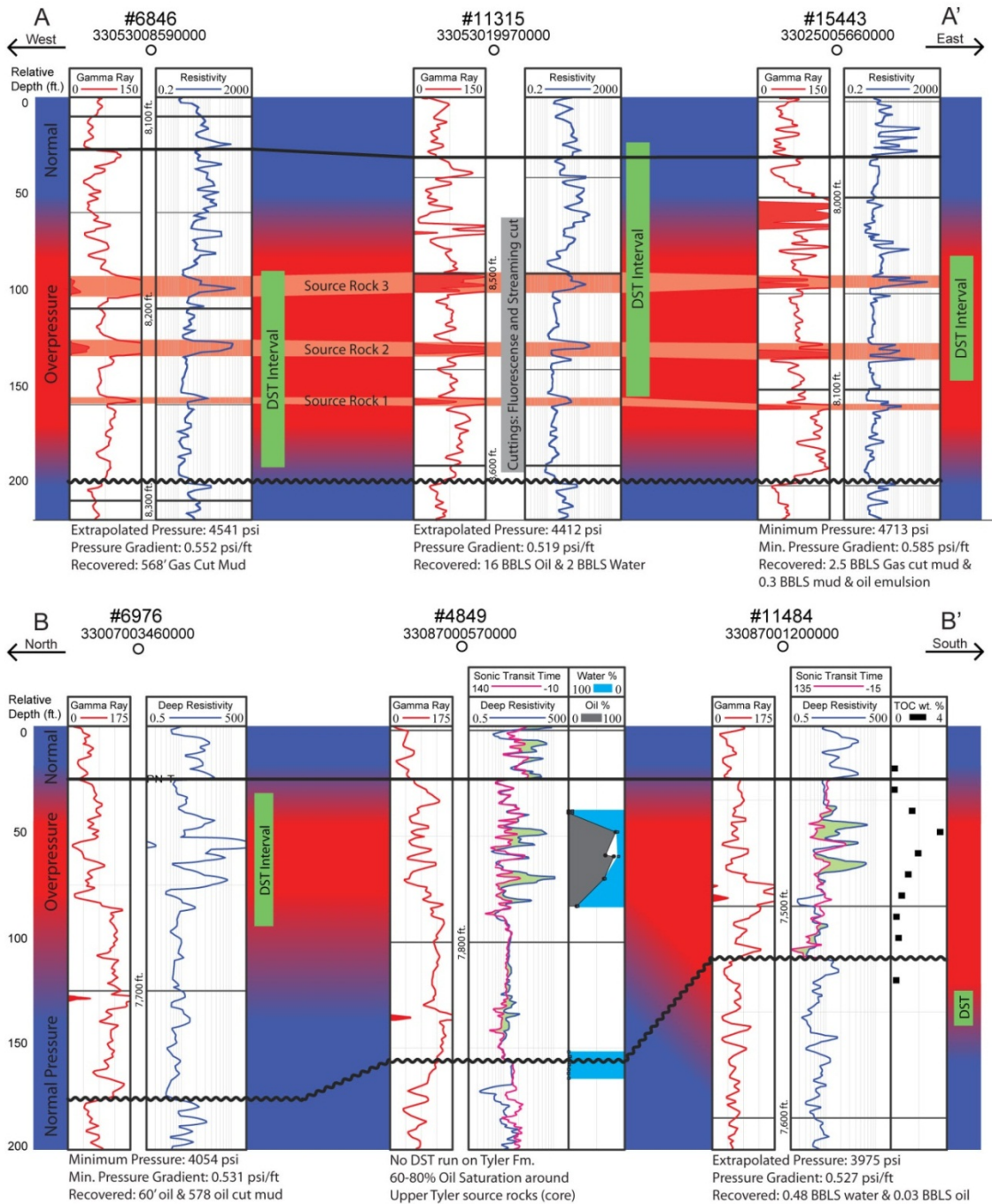
Figure 3.9. Fluid pressure cross-sections of the Tyler Formation with Drill Stem Test (DST), core analysis, and drill cutting information. Red shaded areas represent where the Tyler Formation is oil saturated and overpressured. The blue shaded areas are water saturated with normal fluid pressures. For well #11484 in B-B', the TOC wt. % was measured in drill cuttings sampled at 10 ft. intervals. Resistivity and sonic travel time are cross-plotted to determine where organic-rich intervals may be present within the Tyler section using the method proposed by Passey et al. (1990). The locations of A-A' and B-B' are shown on Figure 3.4.

The Tyler Formation contains fluid overpressure in parts of western North Dakota. Based on fluids recovered during the Drill Stem Tests, the fluid overpressure in the Tyler Formation is likely the result of intense oil generation, which indicates two things: 1) Tyler source rocks are thermally mature and have generated significant amounts of oil and/or gas, and 2) low permeability/porosity layers (seals) enclose the source rocks thereby minimizing oil migration from the Tyler petroleum system/s and inhibiting re-equilibration with the hydrostatic water column. Therefore, oil generated by the Tyler source rocks has accumulated within the Tyler system and has not significantly migrated out of the Tyler system.

There are likely two regions of fluid overpressure within the Tyler Formation: a northern region, located in the deeper parts of the Williston Basin, and a southern region in southwestern North Dakota. These two overpressured regions are separated by areas with normal, hydrostatic fluid pressure. The stratigraphic location and vertical extent of fluid overpressure may vary between the northern and southern regions of overpressure. This variation reflects the difference in Tyler source rocks between the northern and southern petroleum systems.

4. Extraction

The Tyler Formation has produced over 84 million bbls of oil from a total of 285 wells. Tyler production peaked in 1976 when over 3.3 million barrels of oil were produced from 109 wells (see Figure 4.1). Secondary recovery efforts involving water floods began shortly after peak production and continues today. The Tyler Formation has been primarily developed using conventional vertical-well technology that targeted lenticular, oil-bearing, sandstone bodies in southwestern North Dakota (Fig. 4.2).

Oil production from the Tyler Formation was first established early in 1954 from the Dan Cheadle Unit #1 (NDIC #: 518, SE NW, Sec. 9, T139N, R100W). Drilled by Amerada-Hess and Northern Pacific in the Fryburg field, this well initially produced 117 bbls. of oil per day with little water and no gas from a sandstone interval between 8,271 and 8,278 feet depth. This vertical well was hydrofractured with a 7,600 gallon diesel-sand slurry followed by a 3,000 gallon gel-sand mixture. The well was swabbed back and began to flow. According to the North Dakota Industrial Commission, the Dan Cheadle Unit #1 was plugged and abandoned in 1974 after producing 74,691 bbls. of oil and 13,156 bbls. of water from the "Tyler pool". The vast majority of oil production from the Tyler Formation has been from vertical well bores. However, several attempts have been made to increase production through the application of horizontal drilling methods.
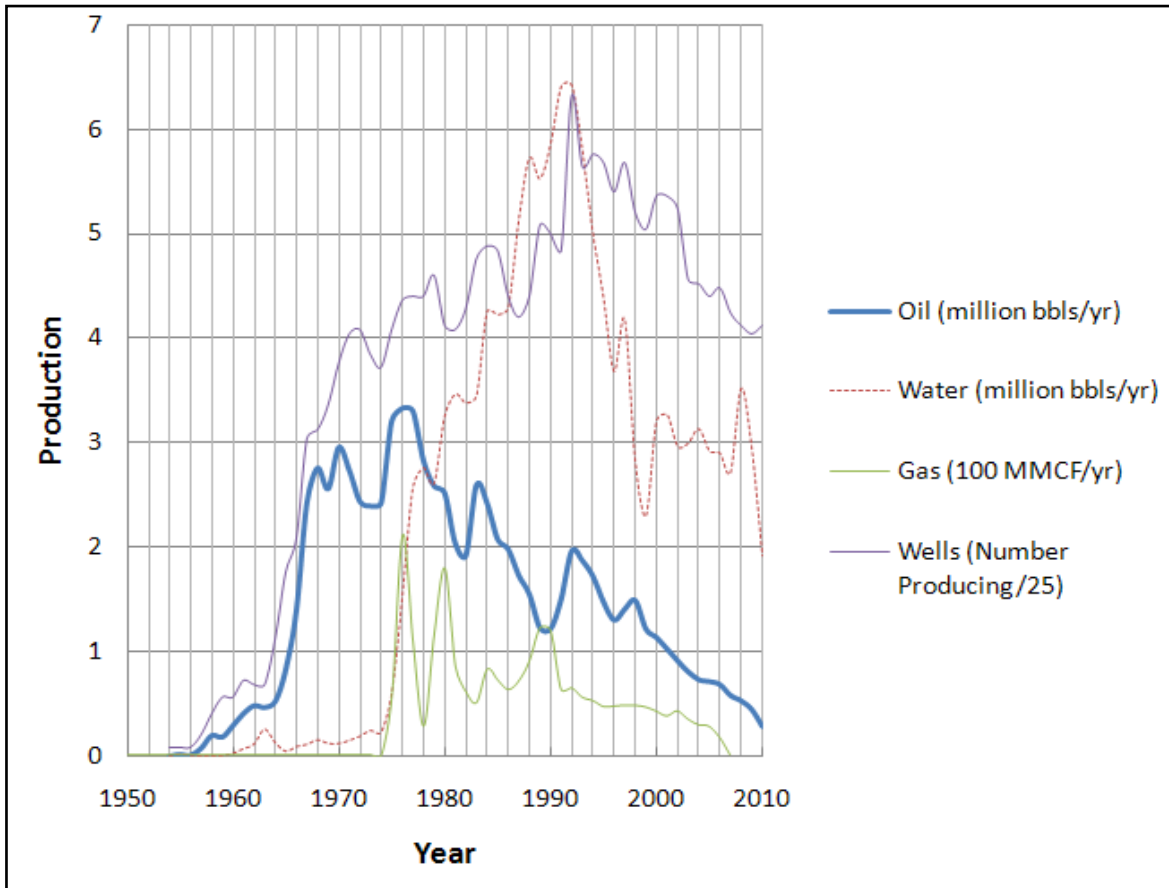

Figure 4.1. Oil production history of the Tyler Formation in North Dakota (from Nordeng, 2011).
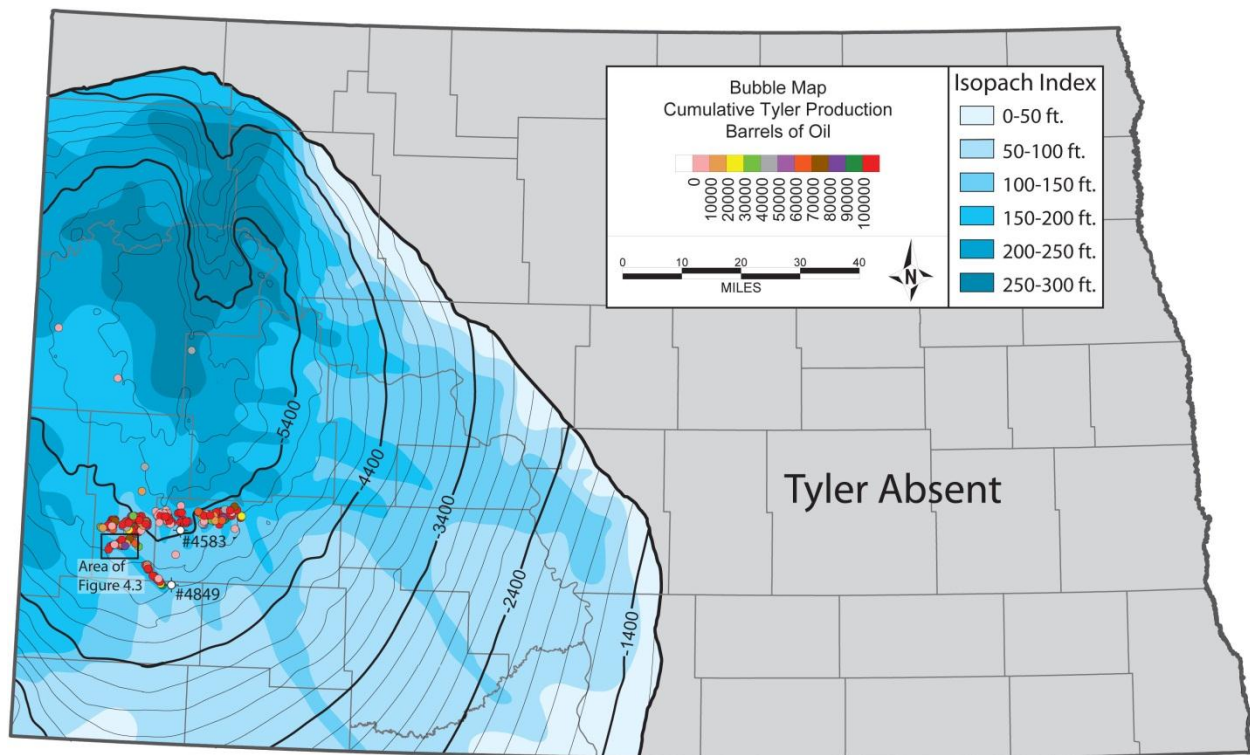
Figure 4.2. Regional map of the Tyler Formation in which the extent is shown by the portion of the map that is not shaded in gray. The contour lines represent the MSL elevation of the top of the Tyler Formation. The shaded contours represent the thickness of the Tyler Formation (modified after Barwis, 1990). Wells that have produced oil are shown as circles with the circle fill color keyed to the wells cumulative oil production. The area shown on the map in Figure 4.3 is contained within the small rectangle that lies near the western limit of known Tyler production.

Horizontal Drilling History of the Tyler Formation

The first horizontal Tyler well was Axem Resources' Tracy Mountain #12-36H (NDIC: 13274, API: 33-007-01271-00-00, W½ SW¼, Sec. 36, T139N, R101W) drilled in the southern portion of the Fryburg field during July 1992 (Fig. 4.3, top right corner). A pilot hole was drilled to a depth of 8,050 feet. The borehole was plugged back to 7,300 feet MD and a horizontal build section was kicked off at a depth of about 7,500 feet with the plan of installing a 3,000 foot horizontal leg in the upper Tyler sandstone at a TVD of 7,923 feet. The pilot hole below the shallowest salt (Picard) and horizontal legs were all drilled with oil based muds. Neither of the laterals in the Tracy Mountain #12-36H managed to reach the expected 3,000 foot mark. Instead the first lateral was shortened to 1,142 feet and a second lateral was drilled some 2,298 feet in length. Both of these lengths are measured from the kickoff point. The shorter horizontal failed to stay consistently within the sandstone so that a variety of lithologies, were encountered. These included 167 feet of the target sandstone with the balance of the well bore penetrating limestone, and shale. The longer lateral encountered more sandstone (1,081 feet) than the

first and was completed with a perforated liner and stimulated with a 47,200 pound sand hydrofracture and a 1,000 gallons of acid (HCl). Initial production (IP) from the Tracy Mountain #12-36 was 32 barrels (bbls) of oil per day with 37 bbls/day of water, and very little gas. This well produced over 1,000 bbls/month of oil for the first few months. However, production tapered off and the well was converted into a water injector after producing 10,456 bbls of oil and 1,544 bbls of water.
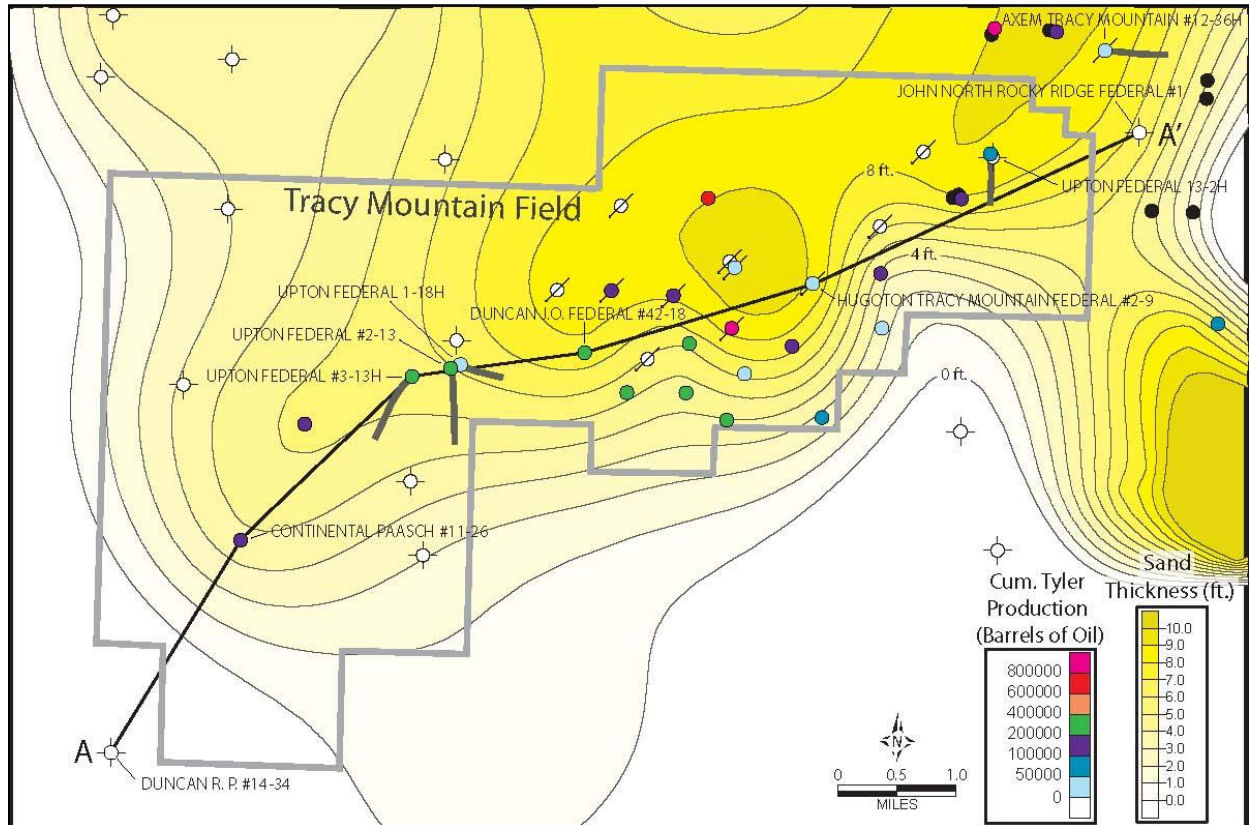

Figure 4.3. Map of the Tracy Mountain field with cumulative Tyler production and the isopach of the productive sandstone interval. The production data used is accurate through May 2011. *Figure 4.2 shows the approximate area and location of Figure 4.3.* A-A' represents the cross-section shown in Figure 4.4.

The Federal #2-13 (NDIC # 15209) was the first economically successful horizontal Tyler well. This well was drilled in the Tracy Mountain field by Upton Resources U.S.A. Inc., in September 2001 (Fig. 4.3). The Federal #2-13 was drilled with an oil base invert mud to the intermediate casing depth. Seven inch intermediate casing was set in the target Tyler sandstone. A 3,063 foot lateral was started, initially using a freshwater mud system. However, a polymer mud system was used to drill the second half of the lateral in an attempt to stabilize the borehole and relieve the tight-hole conditions that hampered drilling. Approximately 85% of the lateral passed through the targeted sandstone interval, occasionally

49

entering the over and underlying shale. The abrasive nature of the Tyler sandstone required six bits to drill the lateral. After drilling, the lateral was treated with enzymes to remove the polymer mud and was left as an open hole with no liner or casing. No additional stimulation was reported. Initial production from the Federal #2-13 was 194 bbls of oil per day with 32 bbls of water and 42 MCF of gas. Since December 2001 this well has produced over 213,000 bbls of oil.

The Federal #3-13 (NDIC# 15261) was the second Tyler horizontal well drilled by Upton Resources (Fig. 4.3 and 4.4). The drilling program was essentially the same as the one used in the Federal #2-13 except that a fresh water polymer mud was used to drill the entire lateral. Five bits were needed to drill the lateral. The lateral was cased with a 4 ½" liner and was treated with an enzyme to remove the polymer mud. The Federal 3-13H initially produced 262 bbls of oil/day, 8 bbls of water/day and 40 MCF gas. To date, the Federal #3-13H has been the most productive horizontal well in the Tyler Formation and has produced more than 300,000 bbls of oil and little water. The Federal #3-13 is still producing 70-80 bbls of oil a day with little water after more than eight years of service.
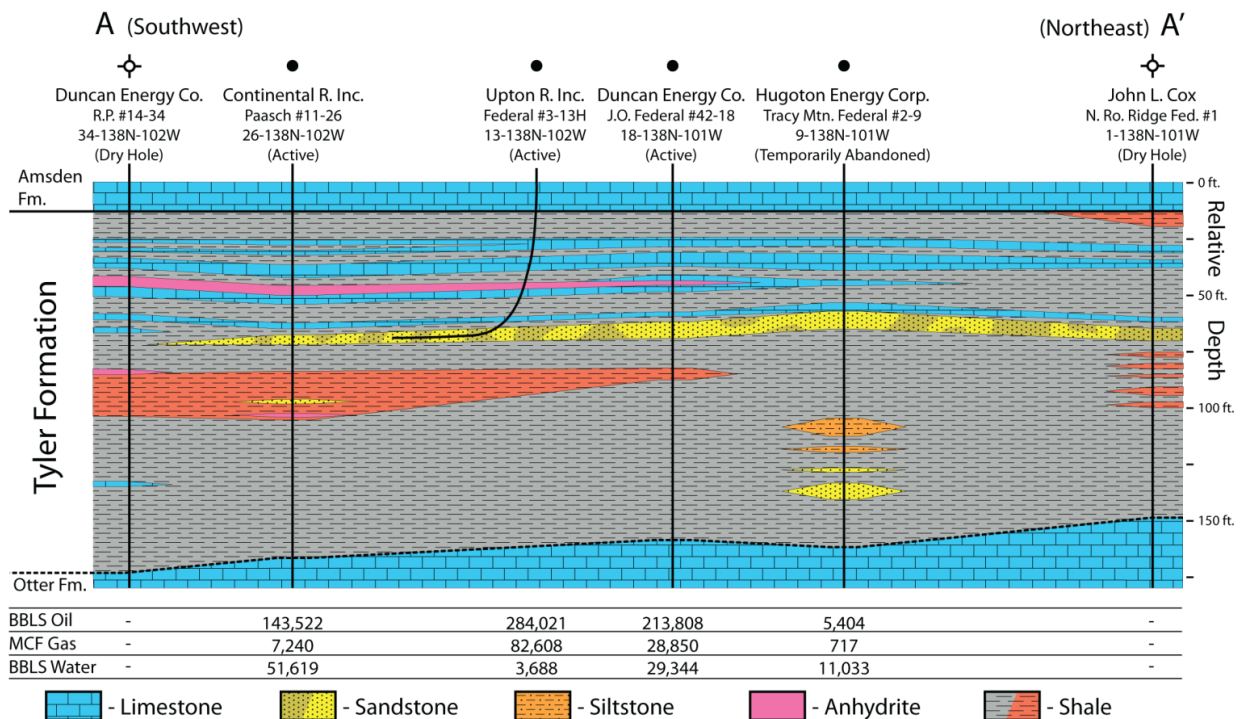

Figure 4.4. Stratigraphic cross-section of the Tyler Formation in the Tracy Mountain field. The cross-section is based on wire line logs and geologic reports on file with the NDIC. The nearly continuous sandstone in the upper portion of the Tyler Formation is the producing interval in the Tracy Mountain field. Lower porosity sandstone intervals are shown in darker shades whereas the lighter colored sandstone areas represent pay zones with well-developed porosity (schematic representation). The curvature and length of Federal #3-13H's borehole is a schematic depiction.

Following Upton Resources early successes, a horizontal re-entry was attempted by Westport Oil and Gas Company. A ~400 foot horizontal lateral was temporarily added to Westport Oil and Gas Company's SFTU #40-22 in August, 2005 (NDIC: 14712, API: 33-007-01385-00-00, SW¼ SE¼, Sec. 22, T139N, R101W). Drilling problems included slow penetration rates, a low angle of inclination upon entering the target zone (73° instead of the intended 85°), and a thin and laterally discontinuous sandstone reservoir. These problems contributed to the wellbore exposing more shale and less sandstone than planned. The lateral was deemed unsuccessful and was plugged and abandoned shortly after being drilled. Even though the SFTU #40-22 has produced over 110,000 bbls of oil from the Tyler Formation, all of this production has been from the vertical portion of the well.

The most recent horizontal Tyler well was Upton Resources' Tracy Mountain Federal 1-18H (NDIC: 16526, API: 33-007-01602-00-00, NE¼ SE¼, Sec. 13, T138N, R102W) that was spudded in March 2007. The Tracy Mountain Federal 1-18H is situated close to two of Upton Resources' earlier horizontal wells (Fig.4.3). The four foot thick target sandstone was found 58 feet below the sample picked top of the Tyler Formation. Difficulty staying within the target sandstone resulted in the borehole straying into the overlying and underlying shale for much of the lateral's length. Drilling of the lateral was terminated before reaching the planned total length because of borehole instability and sloughing. A 4 ½" liner was installed in the lateral and perforated. Even though oil shows were reported throughout the lateral and the sandstone interval was 2 feet high to neighboring wells, the Tracy Mountain Federal 1-18H produced significantly more water (53,256 bbls) than oil (290 bbls) during its brief period of production (Table 4.1).

The success of Upton Resources' horizontal Tyler wells appears to be a function of how consistently the horizontal laterals were able to stay within the targeted sandstone interval. The laterals for both the Federal #2-13 and Federal #3-13H, and the second lateral for Federal 13-2H, were reported to have stayed within the targeted sandstone interval for more than 80% of the lateral's length (Table 4.1). All three of these wells have produced significant quantities of oil (Table 4.1), and Federal #2-13 and Federal #3-13H have had significantly better production histories than the surrounding vertical wells (Fig. 4.5). Federal 1-18H, the least productive well and an economic failure, was not able to consistently stay within the targeted sandstone.
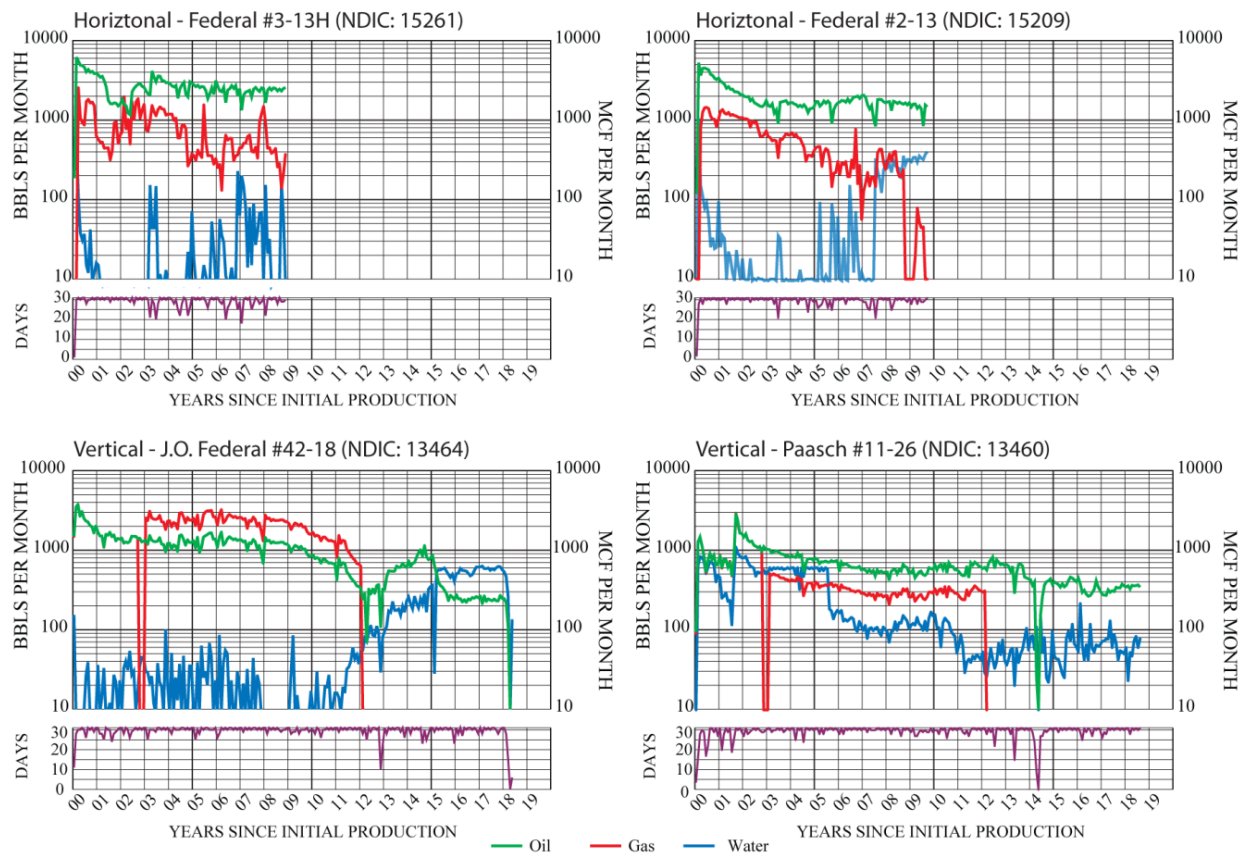
Figure 4.5. Monthly production diagrams comparing vertical versus horizontal well production in the western portion of the Tracy Mountain field. All four wells are shown in Figure 4.3.

Potential Unconventional, Tight Reservoirs

Most of the area where the Tyler Formation contains thermally mature source rocks does not contain much sandstone. So while there is potential in expanding Tyler production using horizontal laterals to target sandstone intervals, there are large, non-sandstone bearing areas where the Tyler Fm. may be oil saturated. Therefore, defining unconventional, non-sandstone reservoir intervals within the Tyler section would be important. One set of potential unconventional reservoirs may be upper Tyler limestones present in southwestern North Dakota. Examples of these limestones are present in wells drilled along the Dickinson-Fryburg trend and near the Rocky Ridge field. Significant oil saturations are present in cores taken from the Gardner #41-9 and Northern Pacific R. R. #22-7.

The Gardner #41-9 was spudded by Shell Oil Company in December of 1969 near Rocky Ridge field (#4583 in Fig. 4.2). Oil production in the Rocky Ridge field is from a channel sandstone deposit that filled an incised valley formed during a sea level low-stand during Tyler time (Hastings, 1990). 163 feet of core was cut in the Tyler Formation and part of the underlying Otter Formation (Fig. 4.6). This well did not penetrate any oil saturated sandstone and was deemed a dry hole. However, of the fourteen core analyses from the Tyler Formation, four limestone samples from the upper part of the Tyler Formation

52

contained between 60-80% oil saturation (Fig. 4.6). Core porosity in these oil saturated limestones ranged from 3-7% with permeabilities of less than 0.1 millidarcies. These limestones are between two and six feet thick and are of comparable thickness to the Tyler sandstone intervals that were horizontally drilled by Upton Resources. Therefore, if these limestones are laterally continuous and oil saturated, they could be potential horizontal targets.

Shell Oil Company's Northern Pacific R.R. #22-7 (#4583, Fig. 4.2) is another well that cored the upper part of the Tyler Formation. Spudded in November of 1968 within the southern part of the Zenith Field, the Northern Pacific R.R. #22-7 cored 45 feet of the upper Tyler Formation (Fig. 4.7). Even though a 3.5 foot thick oil-bearing sandstone was encountered, the sandstone's porosity and permeability were very low and the well was plugged and abandoned. Oil shows (fluorescence and steaming cuts) were not only noted in the sandstone but also in the overlying limestones. Three core analyzes from these limestones contained between 60 to 80% oil saturation. However, the oil saturated limestones contained very low porosity and are poorly permeable.

Several lithologies within the Tyler Formation appear to be correlative between the Gardner #41-9 and Northern Pacific R.R. #22-7.   In particular, the oil saturated limestone intervals in both exhibit low gamma ray responses and high resistivity values (Fig. 4.8). Aligning both wells using the top of the Tyler Formation as datum, at least two of the three oil saturated limestone intervals in the Gardner #41-9, #4849, appear to correlate with oil saturated limestones in Northern Pacific R.R. #22-7, #4583 . Additional shale and underclay/paleosol (green) intervals also appear to correlate. This correlation suggests that there may be a laterally persistent oil saturated limestone interval that may be a regional scale reservoir that extends across the 18 miles that separates these two wells.
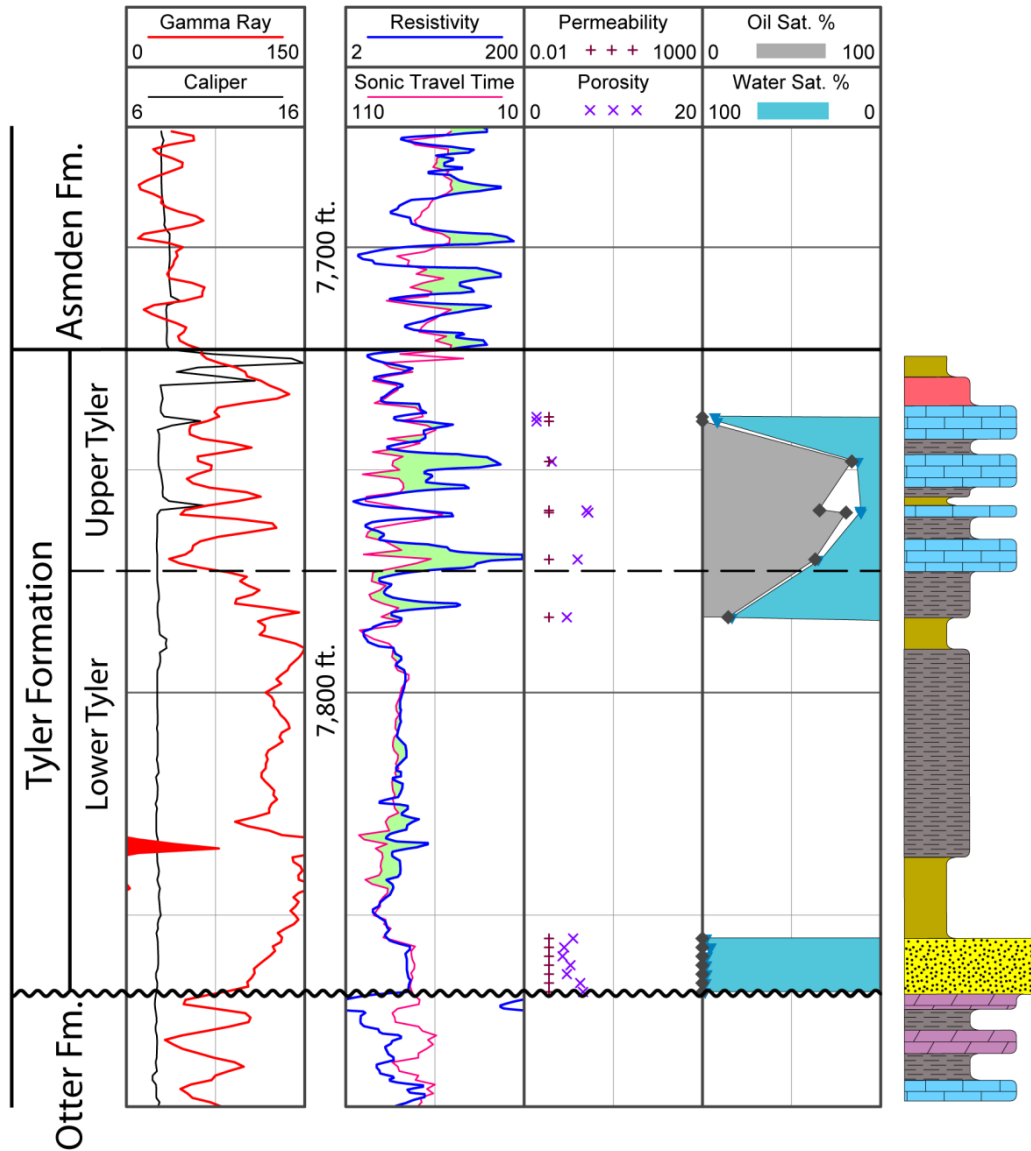
Figure 4.6. Wire line log of Shell Oil's Gardner #41-9. Interpreted core lithologies are displayed to the right. Porosity, permeability, oil saturation, and water saturation are from core analyses. The location of Gardner #41-9 (#4849) is shown in Fig. 4.2.
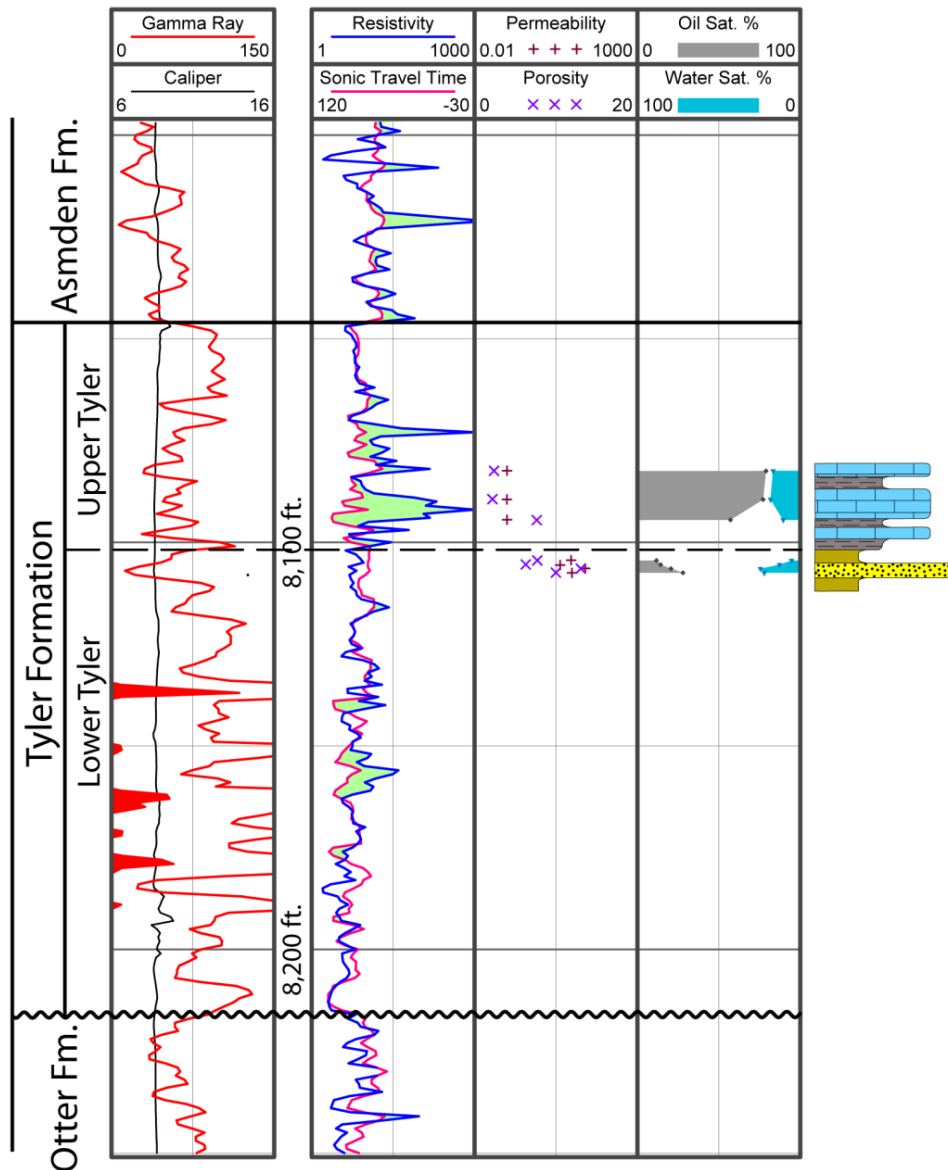
Figure 4.7. Wire line log of Shell Oil's Northern Pacific R.R. #22-7. Interpreted core lithologies are displayed to the right. Porosity, permeability, oil saturation, and water saturation are from core analyzes. The location of North Pacific R.R. #22-7 (#4583) is shown in Fig. 4.2.

Figure 4.8. Correlation of **w**ire line logs between Shell Oil's Gardner #41-9 (#4849) and the Northern Pacific R.R. #22-7 (#4583).   See Figure 4.2 for the location of these wells. The section suggests that there is an oil saturated limestone or limestone dominated interval that extends between these wells.

Table 4.1. Table summarizing drilling information for each of the horizontal Tyler wells discussed here.

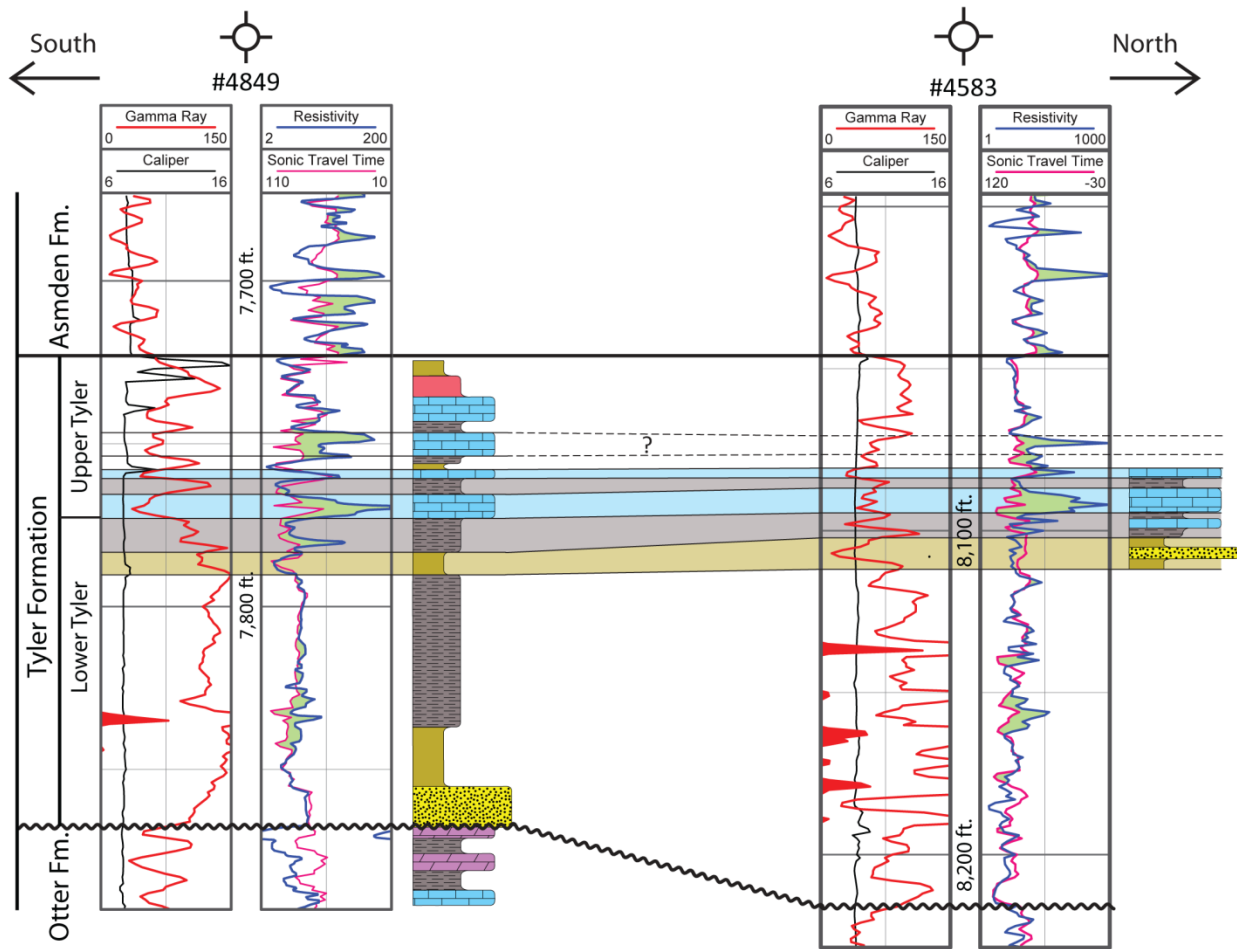| Well Name	NDIC #	Field	Inclination (deg)	Kickoff Depth (ft.)	TVD Target Depth (ft.)	Dogleg Severity (deg/100 ft.)	Lateral Length (ft.)	% of Lateral in Sand	Liner Used	Stimulation	Lateral Hole Diameter (in)	Cum Prod (BBLS Oil)	Well Status
Tracy Mountain #12-36H	13274	Fryburg	86.8	7360	7937	15	1143/2298	<50%/>50%	-	SF, A	7 7/8	10,456	AI
*STFU #40-22	14712	Fryburg	73	7790	8014	32.6	349	<50%	?	-	?	>118,420	A
*Tracy Mountain Federal #12-2	15100	Tracy Mtn	84.7	6931	7952	8.3	131	?	-	-	7 7/8	0	TA
Federal #2-13	15209	Tracy Mtn	86	7662	8222.5	15.3	3063	85%	-	-	8 3/4	>211,000	A
Federal #3-13H	15261	Tracy Mtn	89.6	7636	8223.5	15.3	2526	84%	4.5 in	-	6	>266,789	A
Federal 13-2H	16010	Tracy Mtn	89.2	7138	7951	11	†1440	~100%	4.5 in	-	6	>70,000	A
**Tracy Mountain Federal 1-18H	16526	Tracy Mtn	85.4	7727	8222.5	17.2	1577	<60%	4.5 in	-	6	290	AB

*Horizontal Re-entry: an unsuccessful lateral extension was added to an existing vertical well. The lateral extension was plugged and abandoned.

**Drilling was called on well due to tight hole conditions and fear of losing wells. The target zone was estimated to be 4-6 ft. thick but ended up being only 2-4 ft. thick.

†2nd lateral drilled, 1st lateral hole collapsed

Inclination- The angle (in degrees), in respect to the vertical borehole, of the horizontal lateral upon entering the target zone.

Kickoff depth- The depth at which drilling began to transition from vertical to horizontal.

Dogleg Severity- The rate of curvation as drilling transitioned from vertical to horiztonal.

Perf Record- SF=Stress frac, A=Acid

Well Status: AI= Active water injection well, A= active oil producing well, TA= Temporily abandonded well, AB= abandonded well

Notes: 9 bits were used to drill well #15209's horiztonal lateral and 5 bits for well #15261. "Lateral Length" spans from target penetration to total measured depth.

Table 4.2. 8-year production totals of vertical and horizontal Tyler wells from eastern Tracy Mountain Field.

Well Information			8 Year Cumulative Totals			
Name	NDIC	Well Type	Days	Oil (BBLS)	Water (BBLS)	Gas (MCF)
Paasch #11-26	13460	Vertical	2,825	82,970	42,116	5,817
J.O. Federal #42-18	13464	Vertical	2,847	140,160	2,093	20,654
Federal #2-13	15209	Horizontal	2,830	190,797	4,250	58,824
Federal #3-13H	15261	Horizontal	2,779	257,832	3,248	78,308

References:

Anderson, S. B., 1974, Pre-Mesozoic paleogeographic map of North Dakota: Miscellaneous Map 17, North Dakota Geological Survey, Bismarck, ND.

Barwis, J.H., 1990 Flood-Tidal Delta Reservoirs, Medora-Dickinson Trend, North Dakota, *in* Barwis, J.H., and others, eds., Sandstone Petroleum Reservoirs: New York, Springer-Verlag, p. 389-412.

Blackwell, D. D., Richards, M. C., 2004, The Geothermal Map of North America 2004, American Association of Petroleum Geologists, Tulsa, OK.

Bredehoeft, J.D., Wesley, J.B., Fouch, T.D., 1994, Simulations of the Origin of Fluid Pressure, Fracture Generation, and the Movement of Fluids in the Uinta Basin, Utah: AAPG Bulletin, Vol. 78, No. 11, p. 1729-1747.

Dembicki, H., 2009, Three common source rock evaluation errors made by geologists during prospect or play appraisals: American Association of Petroleum Geologists Bulletin, v. 93, p 341-356.

Dow, W. G., 1974, Application of oil-correlation and source-rock data to exploration in Williston Basin, American Association of Petroleum Geologists Bulletin: V 58, p 1253-1262.

Dorobek, S. L., Reid, S. K., Elrick, M., Bond, G. C., Kominz, M. A., 1991, Subsidence across the Antler foreland of Montana and Idaho: Tectonic versus eustatic effects: Kansas Geological Survey, Bulletin 233, p. 232-251.

Foster, D. I., 1956, N. W. Sumatra Field (Montana), in Judith Mountains – Central Montana: Billings Geological Society, 7th Annual Field Conference Guide book, p. 116 – 123.

Gerhard, L. C., Anderson, S. B., 1988, Geology of the Williston Basin (United States portion): in Sloss, L. L., ed., Sedimentary Cover-North American Craton: U. S., Geology of North America, Geological Society of America, v. D-2, p.221-242.

Gorbachev, V. M., 1975, A solution of the exponential integral in non-isothermal kinetics for linear heating: Journal of Thermal Analysis, v. 8, p. 349-350.

Grenda, J. C., 1977, Paleozoology of cores from the Tyler Formation (Pennsylvanian) in North Dakota, U.S.A.: Unpublished dissertation, University of North Dakota, 337 p.

Hastings, J.O., 1990, Coarse-grained meander-belt reservoirs, Rocky Ridge Field, North Dakota, *in* Barwis, J.H., and others, eds., Sandstone Petroleum Reservoirs: New York, Springer-Verlag, p. 57-84.

Heckel, P. H., 1994, Evaluation of evidence for glacio-eustatic control over marine Pennsylvanian cyclothems in North America and consideration of possible tectonic effects: in Tectonic and Eustatic Controls on Sedimentary Cycles, ed. Dennison, H. M., and F. R. Ettensohn, v. 4.

Hedberg, H. D., 1968, Significance of High-Wax Oils with Respect to Genesis of Petroleum: American Association of Petroleum Geologists Bulletin, v. 52, p 736-750.

Horner, D.R., 1951, Pressure build-up in wells: *Proceedings of Third World Petroleum Congress*, Section II, pp. 503-521.

Hunt, J.M., 1990, Generation and Migration of Petroleum from Abnormally Pressured Fluid Compartments: AAPG Bulletin, Vol. 74, No. 1, p. 1-12.

Hunt, J.M., 1991, Generation and Migration of Petroleum from Abnormally Pressured Fluid Compartments: Reply: AAPG Bulletin, Vol. 75, No. 2, p. 336-338.

Jarvie, D. M., 1991, Factors affecting Rock-Eval derived kinetic parameters: Chemical Geology, v. 93, p 79-99.

Kissinger, H. E., 1957, Reaction Kinetics in Differential Thermal Analysis: Analytical Chemistry.,
v. 29, p 1702-1706.

Lewan, M. D., 1985, Evaluation of petroleum generation by hydrous pyrolysis experimentation: Philosophical Transactions of the Royal Society of London, series A, v. 315, p 123-134.

Lewan, M.D., and Ruble, T.E., 2002, Comparison of petroleum generation kinetics by isothermal hydrous and nonisothermal open-system pyrolysis: Organic Geochemistry, v. 33, no. 12,
p. 1457–1475.

Lopatin, N. V., 1971, Temperatue and geologic time as factors in coalification (in Russian): Akademii Nauk SSSR Izvestiay Serye Geologicheskaya, v. 3, p. 95-106.

Maughan, E. K., 1984, Paleogeographic setting of Pennsylvanian Tyler Formation and relation to underlying Mississippian rocks in Montana and North Dakota; American Association of Petroleum Geologists Bulletin, v. 68, p. 178-195.

Meissner, F.F., 1978, Petroleum geology of the Bakken Formation Williston Basin, North Dakota and Montana: *in* D. Rehig, ed., 1978 Williston Basin Symposium: Montana Geological Society, Billings, Montana, p. 207-227.

Nordeng, S. H., 2012, Basic geochemical evaluation of unconventional resource plays: Geo News, v. 39, p. 14-18.

Nordeng, S.H., 2011, Reviewing the resource potential of the Pennsylvanian Tyler Formation: Geo News, v. 38, no. 1, p. 21-25.

Nordeng, S. H., LeFever, J. A., Anderson, F. J., Bingle-Davis, Johnson, E.H., 2010, An examination of the factors that impact oil production from the middle member of the Bakken Formation in Mountrail County, North Dakota: Report of Investigation No. 109, North Dakota Geological Survey, 85 p.

Oba, M., Hajime, M., Shimoyama, and A. Shimoyama, 2002, Determination of activation energy and pre-exponential factor for individual compounds on release from kerogen by a laboratory heating experiment: Geochemical Journal, v. 36, p 51-60.

Passey, Q. R., Creaney, S., Kulla, J. B., Moretti, F. J., Stroud, J. D., 1990, A practical model for organic richness from porosity and resistivity logs: American Association of Petroleum Geologists Bulletin, v. 74, p. 1777-1794.

Peters, K.E., and Cassa, M.R., 1994, Applied source rock geochemistry, *in* Magoon, L.B., and Dow, W.G., eds., The petroleum system—From source to trap: Tulsa, Okla., American Association of Petroleum Geologists Memoir 60, p. 93-117.

Peterson, J. A., 1981, General stratigraphy and regional paleostructure of the western Montana overthrust belt, in Tucker, T.E., ed., Field Conference and Symposium Guidebook, Southwest Montana: Montana Geological Society, p. 5-35.

Schmoker, J. W., 2002, Resource-assessment perspectives for unconventional gas systems, American Association of Petroleum Geologists Bulletin: V 86, p. 1993-1999.

Schlumberger, 2011, Oilfield Glossary, http://www.glossary.oilfield.slb.com/Display.cfm?Term=drillstem %20test (Retrieved 20 July 2011).

Sturm S. D., 1987, Depositional history and cyclicity in the Tyler Formation (Pennsylvanian), Southwestern North Dakota, in Longman, M.W., ed, Williston Mountain Association of Geologists, p. 209-221.

Suuberg, E. M., W. A. Peters, and Howard, J. B., 1978, Product composition and kinetics of lignite pyrolysis: Industrial Engineering and Chemical Processes Design and Development, v. 17, p. 37-46.

Tissot,B., and Espitalie', 1975, L'evolution thermique de la matiere oranique des sediments: applications d'une simulation mathematique: Revue de l'Institut Francais du Petrole, v. 30, p. 743-777.

Toth, J., Maccagno, M.D., Otto, C.J., and Rostron, B.J., 1991, Generation and Migration of Petroleum from Abnormally Pressured Fluid Compartments: Discussion: AAPG Bulletin, Vol. 75, No. 2, p. 331-335.

Williams, J. A., 1974, Characterization of oil types in Williston Basin: American Association of Petroleum Geologists Bulletin: V 58, p 1243-1252

Willis, R. P., 1959, Upper Mississippian-Lower Pennsylvanian stratigraphy of central Montana and Williston Basin: American Association of Petroleum Geologists, v. 43, p. 1949-1966.

Wood, D. A., 1988, Relationships between thermal maturity indices calculated using Arrhenius equation and Lopatin method: implications f or petroleum exploration: American Association of Petroleum Geologists Bulletin, v. 72, p 115-134.

Ziebarth, H. C., 1962, The micropaleontology and statigraphy of the subsurface "Heath" Formation (Mississippian-Pennsylvanian) of western North Dakota: unpublished M.S. thesis, University of North Dakota, 145 pp.